Event Detection in EEG signals for Brain Computer Interface using Expectation-Maximization Algorithm

A Thesis
Submitted in Partial Fulfiment of The Requirement
for The Award of The Degree of
MSc in Biomedical Engineering

by

LIJO VARUGHESE CHACKO

Department of Biomedical Engineering
University of Strathclyde
Glasgow, United Kingdom
2011-2012

Declaration

'This thesis is the result of the author's original research. It has been composed by the author and has not been previously submitted for examination which has led to the award of a degree.'

'The copyright of this thesis belongs to the author under the terms of the United Kingdom Copyright Acts as qualified by University of Strathclyde Regulation 3.50. Due acknowledgement must always be made of the use of any material contained in, or derived from, this thesis.'

Signed:

Date:

Acknowledgement

My sincere thanks are due to a lot of people without whose help and support, this study would never have been a reality.

I am honour-bound to express my heartfelt gratitude to my Project Supervisor, **Dr. Heba Lakany**, for her guidance, which has been of inestimable value for the maturation of my project.

With an overwhelming heart, I thank **Prof. Helen Grant**, for her unfailing encouragement during my difficult times, and for making it possible for me to improve a lot under the aegis of the Department during the course of my study. I express my sincere thanks to all the members of the Department of Biomedical Engineering for their constant inspiration and support all through my academic pursuit.

I thank all my classmates and friends who have always been there with me to happily extend a helping hand when I was in need for some aid. Special thanks are due to my best friend **Ms. Belga Marriya Berk** for instilling confidence in me whenever I were about to lose heart during the toughest days. She also did the proofreading of my thesis.I also thank **Mr.Ange Tano** for backing me with his excellent programming skills.

I wholeheartedly thank **Pastor Babu Zachariah** and his family and all the members of **Ebenezer Pentecostal Church** for their sincere prayers and care during my days of illness. Also, let me remember the Doctors, Nurses and other staff members of Glasgow Royal Infirmary with a grateful heart.

The gratitude, which I feel for my family, for motivating me and for coming up with timely suggestions, is beyond words. However, let me make a vain attempt here to thank them.

Above all, I am indebted to **God Almighty** for His grace upon me.

Abstract

Past two decades have witnessed a steady growth in research related to Brain Computer Interface (BCI), which offers a non-muscular communication pathway to patients disabled due to neurological disorders. BCI works by recording brain signals (example; electroencephalography (EEG)) and translating them into machine-understandable language. Most of the current BCI systems identify features of the brain signals and classify them according to a predefined criterion set by the classifying algorithm. The features of the brain signals can change over time and this could adversely affect the feature extraction and classification algorithm. This restricts the use of BCI in a laboratory oriented device.

Due to these impediments, this study aims at detecting events in EEG signals rather than classifying them. As detection would not require classification of the features, the process is less susceptible to changes in signal features. Thus, it could be possible to bring BCIs into clinical use. The current study modelled the features of rest EEG signal using a Gaussian distribution and a mixture of Gaussians. The features of EEG were extracted using continuous wavelet transform and the parameters of the models were estimated using an Expectation-Maximization (EM) algorithm. Maximum-likelihood estimates of the parameters of the rest EEG and EEG during motor actions were compared.

Statistical analysis of the results indicates that there are differences between maximum-likelihood values of the wavelet coefficients of the rest EEG and EEG undergoing motor activity. Two models of Gaussian mixture gave better results than a simple Gaussian distribution. This shows that Gaussian mixture modelling (GMM) of EEG is sensitive enough to depict changes during motor activity with respect to rest EEG.

Contents

List of Figures

List of Tables

List of Abbreviations

ALS	Amyotrophic Lateral Sclerosis
BCI	Brain Computer Interface
CAR	Common Average Reference
CRT	Cathode Ray Tube
CWT	Continuous Wavelet Transform
DWT	Discrete Wavelet Transform
ECoG	Electrocorticogram
EEG	Electroencephalogram
EM	Expectation-Maximisation Algorithm
ERD	Event Related Desynchronization
ERP	Event Related Potential
ERS	Event Related Synchronization
ERSP	Event Related Spectral Perturbation
FFT	Fast Fourier Transform
fMRI	Functional Magnetic Resonance Imaging
FT	Fourier Transform
GMM	Gaussian Mixture Modelling
ICA	Independent Component Analysis
ITC	Inter Trial Coherence
ITR	Information Transfer Rate

LCD	Liquid Crystal Display
LED	Light Emitting Diode
LLH	Log-likelihood
LSP	Language Support Program
MEG	Magnetoencephalography
MI	Motor Imagery
PCA	Principal Component Analysis
PET	Positron Emission Tomography
SCP	Slow Cortical Potential
SMR	Sensorimotor Rhythm
SSVEP	Steady State Visual Evoked Potential
STFT	Short Time Fourier Transform
TTD	Thought Translation Device
TVEP	Transient Visual Evoked Potential
VEP	Visual Evoked Potential
WT	Wavelet Transform

1 Introduction

Human brain is more complex and sophisticated than the brain of any other organism in the entire living kingdom. Our brain controls and coordinates all the processes and functions in our body without any conscious effort. Brain communicates through the spinal cord and other neural networks in our body. Disorders such as multiple sclerosis, amyotrophic lateral sclerosis (ALS), cerebral palsy, brainstem stroke, muscular dystrophies and brain and spinal cord injuries impair the natural communication pathway between brain and other parts of the body[1]. Severe disorders can cause complete impairment of the neuronal pathways to muscles, which sometimes leads the person to a locked-in state[2, 3]. In a locked-in condition, the patient cannot move or communicate with the external world. However, the patients can survive with the help of life supporting equipments and other individuals.

Brain Computer Interfaces (BCIs) are devices which are capable of controlling artificial devices using the signals taken from the brain. They provide a non-muscular communication channel for patients who are in locked-in condition[4]. BCIs can be employed for restoring sensory functions, for stimulating communication with the external world, for controlling prosthetic devices like wheelchairs[5] and robotic arms etc[6].However, BCIs are often used as interfaces for controlling artificial devices by processing signals taken from the brain. BCIs works in real-time, i.e., signals from the brain are processed on-line and converted into machine understandable language. Hence the intention behind the concept of BCI is to translate the intention of a person into machine language by using brain signals[7].

There are several techniques available to obtain information about the ongoing processes in the human brain.Electroencephalography (EEG), Magnetoencephalography (MEG), Positron Emission Tomography (PET), functional Magnetic Resonance Imaging (fMRI) and Optical Imaging are the prominent techniques to monitor the brain's activity. However, MEG, fMRI and PET methods are not efficient for rapid communication since they depend on blood flow and that makes them less favourable for BCI related uses[4]. Presently, the most widely used method to measure brain activity for BCI is EEG signals. The reason for using EEG signals for BCI are less expense, portability, less time consumption and adaptability to almost

all environments[8]

1.1 Aim of the Study

BCIs work by identifying features of the EEG signal and translating them into device commands. Most of the BCI systems work by classifying the extracted features during the signal analysis. There are possibilities that as time passes the features of the EEG signals from the user might change. These changes will adversely affect the accuracy of the classification system in the BCI. Moreover, BCI systems are bound to laboratory environment due to noise considerations and complexity of BCI system. To make BCIs work in household conditions, simpler yet reliant signal processing techniques are needed. Detection of brain events (eg: ERD/ERS, SSVEP) without classification might serve to overcome the above stated problem. This would allow simple one dimensional selection task and it would be more reliable than classification in a domestic environment.

The aim of this study is to develop an event detection technique by modelling the features of rest EEG data into Gaussian Mixture Model (GMM) and comparing it with GMM of EEG during motor task. It is hypothesized that the parameters of Gaussian model of EEG under rest and EEG under motor task might elicit some difference. These differences in parameters of the model will help in identifying the time and duration of the events in EEG.

1.2 Structure of the Thesis

This chapter will be followed by chapter two which presents an overview of current BCI systems based on EEG signals. Chapter three and four will discuss the event detection in EEG and different feature analysis techniques . Chapter five gives the experiment design and methodology of the project. Chapter six will present the results obtained in the study. Chapter seven will discuss the results. Final chapter concludes the thesis and discusses the scope of the study.

2 EEG and Brain Computer Interface

EEG represents the electrical activity of neurons in the brain. In 1979, Hans Berger presented the very first paper on EEG and from then on, EEG has been used as a diagnostic tool to evaluate the functions of the brain. EEG reflects the ongoing activities in the brain. Hence, theoretically, EEG could be used to decipher human thoughts[4]. Thus, the information from the EEG waves could help to develop a brain computer interface. However, predicting the exact intention of the person from EEG is quite complex due to the huge number of neurons in the brain. Brain is controlling all the organs, functions, processes and everything in the body and so, EEG reflects every action that is happening inside the body. A BCI system should extract features of physical events (eg: motor activity) from the EEG signal. To isolate a single physical event from the analysis of EEG is not an easy task. However, advancements in EEG signal processing and better electrode technologies would help improve to extract accurate information about physical events from EEG signal.

One important aspect of EEG is the knowledge about the rhythms in EEG wave. With the advancement in technology, immense research has been done with a view to finding the relationship between the brain waves and their origin and mechanism. Various experimental studies have made clear the relationship between EEG signals and mental tasks[9, 10]. There is a fair amount of information available for researchers which would facilitate the use of EEG as a source to drive BCI. Also, with better hardware resources and signal processing algorithms, now it is possible to analyse and process multichannel EEG. Hence, it is possible to setup more complex BCI systems like word speller[11] and prosthesis control[6]. The research on BCI will help to improve the quality of lives of people suffering from neurological disorders and spinal cord injuries.

Several methods are currently available to record EEG signals using electrodes, which include epidural, subdural and scalp-recorded EEG activity. The first two methods are invasive but give higher resolution and amplitude than scalp-recorded

EEG. Subdural electrodes or intracortical electrodes provide greater resolutions than other methods and can even obtain single neuron potentials[12, 8]. However, these invasive methods raise the risks of infection and also require more challenging clinical interventions, and so they are less favourable options for BCI. Surface EEG has less resolution and amplitude in comparison with the invasive methods. Despite these shortcomings, it is comparatively safer and less expensive. Under application of suitable signal processing techniques, it is possible to extract a fair amount of information to drive a BCI system.

2.1 EEG Recording

Usually an EEG recording setup consists of electrodes, instrumentation amplifiers, analog-to-digital converter and a recording device. The electrodes convert ionic potential into electrical potential which is fed into the amplifier for amplification. The amplified signal is converted into digital format by the analogue-to-digital converter. Digital signals are understandable to the computers and can be manipulated with the computer system.

The measurement of EEG signals requires an active electrode, a reference electrode and a ground electrode. The potential difference between active electrode and reference electrode is measured using a differential amplifier with respect to the ground electrode. BCI requires an array of electrodes to extract information required to record the intentions of the individual. Currently available EEG measurement systems are configured to use up to 120 to 220 electrodes which are usually made of silver chloride. Impedance level between electrode and the scalp should be between 1 kΩ and 10 kΩ in order to make an accurate measurement. To make a better contact and to reduce contact impedance, electrode gels are widely used[13].

The amplitude level of EEG signal is in the range of microvolts only and so, it requires high amplification level for further processing. These low amplitude signals are prone to noises such as 50 Hz power-line interferences and other electronic noises. Furthermore, during recording, EEG could be mixed with motion artifacts and muscle activity. The design of the EEG system must consider these noises and steps should be taken to avoid them.

2.1.1 Electrode Placement and Referencing

The placement of electrodes over the scalp are according to the 10-20 international lead system[14]. Two reference points are determined on the head in order to place the electrodes. One of the reference points is the inion, which is at the back of the skull and the other reference point is the nasion, which is just above the nose. The skull is divided by the transverse and median planes with respect to the reference points. The locations of electrodes are determined by dividing these planes at intervals of 10% and 20%. Electrode locations are named according to the specific brain regions in such a way that the letters C, F, O, P, P_g and F_p represent central, frontal, occipital, parietal, nasopharyngeal and frontal polar regions respectively. Electrode placements are shown in figure 2.1.

The voltage of the active electrode is measured with respect to a reference electrode. However, if there is any activity happening in the site of the reference electrode, it will influence the measurement. Two methods of referencing are widely used for EEG measurement i.e., common reference site and common average referencing. Common reference site, which is the popular method, takes the electrode placed on the nose or mastoid as the common reference. However, in high density EEG measurements, this method is not recommended because it influences the actual measurement. To circumvent the referencing problem in high density measurements, common averaging technique is recommended.Average referencing system takes the average of all the electrode measurements except that of the active electrode[15].

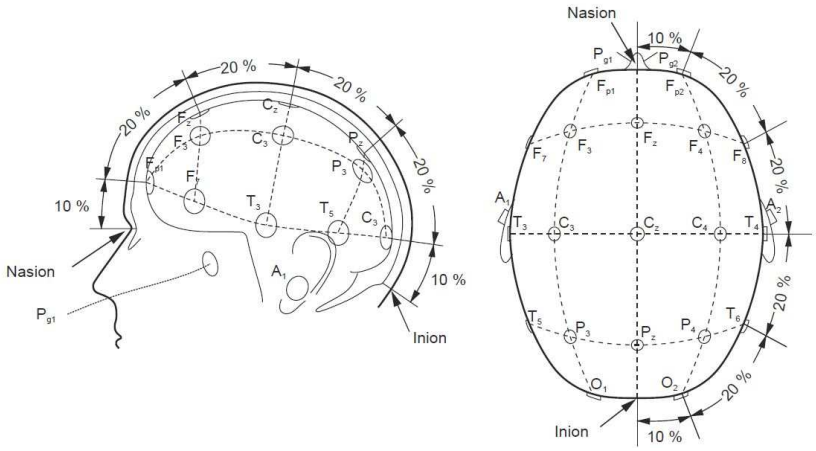

Figure 2.1: Electrode Placement Over Scalp. The figure in the left and right shows the side view and top view of the locations of electrode placement over the scalp respectively. The electrode locations are marked according to 10-20 international lead system. Reference points (Nasion and inion) are highlighted with a pointer.[13]

2.2 Control Signals in BCIs

Brain signals contain information about different tasks that are currently performed by the brain. Albeit physiological significance and the origin of most of the brain signals are still being studied, it is now possible to decode some of the brain signals to understand the user intentions. These signals which are capable of controlling BCI systems are called control signals. Most widely used control signals in current BCI systems are P300 Evoked Potentials, Visual Evoked Potentials, Slow Cortical Potentials and Sensorimotor Rhythms.

2.2.1 P300 Evoked Potentials

P300 evoked potentials are positive high peak wave forms which are produced in the EEG during infrequent auditory, visual or somatosensory stimuli. These peaks are elicited about 300ms after getting an oddball stimulus among frequent stimuli[11]. It is mostly observed in the parietal and central regions of the brain. The advantage of using P300 response as a control signal is that it does not require

user training. However, the amplitude of the response gets eventually reduced due to familiarization with the infrequent stimulus. To avoid this situation, rare stimuli are presented randomly. BCI using P300 evoked potentials as control signals will be explained in the next chapter.

2.2.2 Visual Evoked Potentials

Visual Evoked Potentials (VEPs) are generated at the visual cortex of the brain after receiving a visual stimulus. The amplitude of the VEP increases when the stimuli move closer to the central visual field. VEPs are classified into three different classes according to three different criteria: (i)the morphology of visual stimulus, (ii)the frequency of visual stimulation and (iii) field stimulation[16]. According to the morphology of the visual stimulus, VEPs can be evoked by presenting the subject with a flash stimuli or using specific graphic patterns such as checkerboard lattice, gate and random-dot map. The second criterion is based upon the frequency of visual stimulus and VEPs generated under this criterion are classified as transient VEPs (TVEPs) and steady-state VEPs (SSVEPs). SSVEPs happen only in higher frequencies of visual stimuli while TVEPs elicit only when the frequency of visual stimuli is below 6 Hz [17]. The third criterion divides VEPs based on the area of on-screen stimulus. Depending upon the area of on-screen stimulus, VEPs are divided into whole field, half field and part field VEPs.

VEP response varies with the stimulus provided. For instance, flash TVEPs produce a series of negative and positive peaks with prominent peaks at 90 ms and 120 ms respectively, while pattern onset/offset causes two positive and one negative peaks[18].

SSVEPs are produced by the same stimulus as explained above. However, the frequency of the stimulus provided should be above 6 Hz. The amplitude of the main peak and its first and second harmonics of the SSVEPs increase when the user gazes at the flickering target. The frequency of the peaks would be the same as the frequency of the stimulus[19]. In contrast to TVEP, the phase and amplitude of the frequency components of SSVEP remain constant over longer periods of time. Furthermore, SSVEPs are less susceptible to the artifacts caused by the movements of eye and electromyographic noises than TVEP. Hence, SSVEP based BCIs are

more common than TVEP based BCIs[13].

2.2.3 Slow Cortical Potential

Slow Cortical Potentials (SCPs) are the slowest changing potentials among the low frequency components (at around 1 Hz) of the scalp recorded EEG[20]. SCPs occur due to the activity of the cortical region of the brain. Usually potential shift happens in an interval of 0.5s to 10s, hence the name slow cortical potential[21]. The advantage of SCP is that it can be regulated by the user himself with proper training and practice. Negative SCPs represent increased neuronal activity, while positive SCPs show decreased activity of cortical neurons. User can be trained to regulate the SCP voluntarily with the help of proper feedback. Self-regulation of SCPs depends upon several factors such as subject's psychological and physical state, motivation, social context and subject-trainer relation, sleep, and pain[22].

2.2.4 Sensorimotor Rhythms (SMR)

These are rhythms measured over somatosensory cortices of the brain. Sensorimotor rhythms include μ-rhythm with a frequency around 10 Hz (8-11 Hz), usually combined with β-rhythm (around 20Hz) and γ- rhythm (around 40Hz). Some of the β-rhythms are harmonics of the μ-rhythms and some components might appear independent as well. Several studies show that SMR leaks to the parietal electrodes and it is also visible in patients with amyotrophic lateral sclerosis[23]. The amplitude of the SMRs varies with the motor tasks. One of the most interesting fact about SMR is that, actual movement is not required to cause changes in the sensorimotor rhythms. The subjects can imagine the motor task and with the imagination, modulation of SMR is possible. This advantage of SMR makes it a favourable option, as a control signal, for patients who are in locked-in condition. Amplitude of sensory motor rhythms tends to decrease or desynchronize during actual movement or motor imagery and the amplitude will increase or synchronize after the movement or during relaxation time[24]. Despite the degeneration in cortical and spinal motor neurons, it is possible to modulate the SMR[23]. However, when compared with healthy subjects, amplitude of SMR is low in patients with ALS.

2.3 A Review of Current BCI systems

This section presents a literature review of current BCI systems.

2.3.1 Types Of BCIs

Based on control signals used, BCIs can be classified into exogenous and endogenous systems[13]. In exogenous BCI, signal changes in the EEG require external stimuli such as visual or auditory stimulus. P300 and VEPs are examples of exogenous response. Main advantage of exogenous BCI is that, it does not require extensive training. Moreover,it also features high data rate.In endogenous BCI system, the user learns to self-regulate brain rhythms without any external stimulus. This BCI system is based on endogenous signals like sensorimotor rhythms and SCPs. The benefit of endogenous system is that, patients with visual impairment or ALS could self regulate their brain rhythms and can be able to control BCI. In the coming sections, a review of both exogenous and endogenous BCI systems will be presented.

Based on input processing technology, BCIs are classified into synchronous and asynchronous systems[13]. Synchronous BCI process input signals only during predefined time windows i.e., any input will be ignored outside this time window. The advantage of synchronous system is that the patient can make conscious efforts in order to control the BCI system, thus avoiding processing of misleading events such as eye blinks and motion artefacts. Asynchronous BCI continuously processes the input data which offer a natural man machine interface. However, this kind of system is very complex and demands more computational power.

Here, the BCI systems are explained on the basis of control signals and mentions the input processing technology used, where ever appropriate.

2.3.2 P300 Based BCI

In 1988, a paper published by Farwell and Donchin[11] showed that P300 component in the EEG signal can be used to select characters presented in a computer screen. In their experiment, the user was presented with a 6×6 matrix of numbers or symbols and in every 125ms a row or column would be highlighted with a flash

of light. In a complete trial, each column and row would be flashed twice. The user was asked to select a particular symbol from the matrix. The target would only flash twice during a sequence of 12 flashes, hence producing two rare events out from the 12 flashes which elicit P300. EEG was picked from parietal cortex and was digitized to take the average response to be compared between that of each row and column. Amplitude of the P300 was compared in all possible combinations. Only the desired selection of user's symbol had shown the maximum amplitude P300. This was used to detect the intention of the user. One of the advantages of P300 is that it does not require any initial training of the subject.

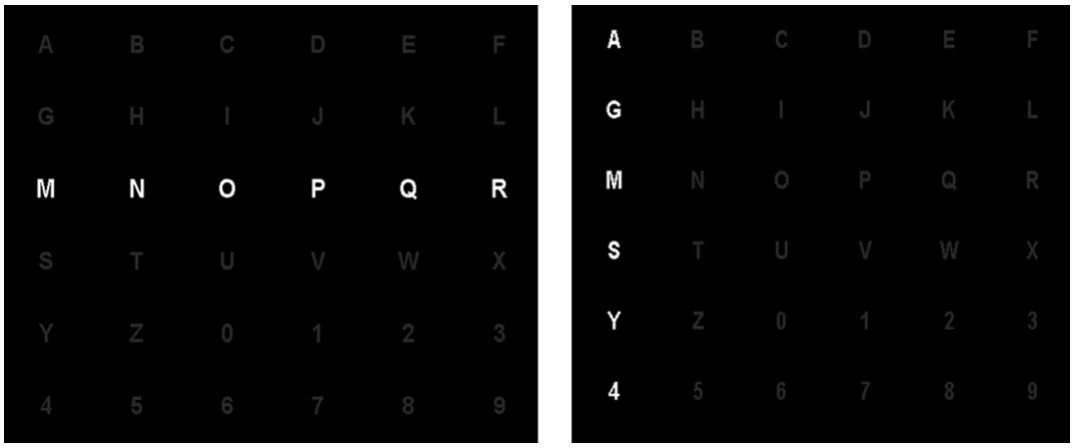

Figure 2.2: A typical 6×6 matrix for P300 speller BCI. (left) Matrix highlighting a column of characters. (right) Matrix highlighting a row of characters. During the trial, rest of the characters are invisible[25].

Many researches have been done on P300 as a speller device. The intention of the ongoing studies are to improve the classification rate and accuracy of the prediction. A study report published by Thulasidas et al. shows that, online classification of 3 characters per minute with 95% accuracy is possible with a vector machine classifier[26]. ALS patients are also able to use P300 as input to the BCI, which was first demonstrated by Sellers et al. They compared the efficiency of P300 as inputs for BCI among healthy and paralyzed subjects and found that healthy subjects performed better than paralyzed subjects[27], provided that both the groups underwent the experiment without any initial training.

2.3.3 SSVEP Based BCI

SSVEP based BCI system comes under the category of exogenous BCI. Like P300, this type of BCI requires gaze to a visual stimulus. However, instead of the requirement of rare stimulus to elicit P300, SSVEP requires flickering visual stimuli. To present the user with different frequencies of flickering targets, an LCD/CRT monitor[19] or a board with LED[28] is widely used. In 2002, Cheng et al., developed an SSVEP based BCI to input telephone numbers[29]. This system consists of virtual keypad with 13 characters displayed in a CRT monitor with a refresh rate of 70.14 Hz. Only two channels (O1 and O2) were taken for processing the EEG. FFT of the EEG signal was performed for every 0.3 seconds. Amplitude of SSVEP response was calculated by summing up the amplitude of fundamental frequency and its second order harmonics. This amplitude was compared with a set threshold in order to register the selection of user's intended key. 8-13 subjects managed to dial the intended phone number. The average transfer rate of this experiment was 27.15 bits/min. In 2006, the same group[19] tried to reduce inter-subject variability by choosing channel locations and frequency of the stimulus and obtained an increased transfer rate of 43 bits/min.

A recent study by Volosyak et al., developed an SSVEP based spelling device that achieved a transfer rate of more than 100 bits/min[30]. They have introduced changes in signal processing and graphical user interface which made them to achieve higher information transfer rate. Frequency detection from spatially filtered signal had been done by using the power of the stimulating frequency and its harmonics instead of signal-to-noise ratio in other methods. In their study, the user was presented with a virtual keyboard with 32 characters in an LCD screen with refresh rate of 120 Hz. The screen consisted of five selection keys placed around the edges. Each selection key was presented in a white box and all had different flickering frequency. The selection keys included 'select' (6.67 Hz), 'left' (7.5 Hz), 'right' (8.57 Hz), 'up' (10Hz), and 'down' (12 Hz). The user could move the cursor by selecting the navigating keys and the selection could be made by selecting the 'select' key. The system also provided the user with an audio feedback when the user made a selection.

The primary requirement of SSVEP based BCI is intact gaze on the stimuli, thus impeding the use of SSVEP in patients with less eye movement control. Kelly

et al. compared the classification accuracies when subjects did not require to gaze at the flickering stimulus. Instead, they had to concentrate on a fixation cross between targets. The authors referred this condition as covert attention[31]. The results of the classification rate shows a reduction in accuracy from 90% to 70%, of the covert attention when compared with the fixed gaze. This shows that a simple two target SSVEP could be used for people who are in locked-in condition despite low accuracy in classification rate.

2.3.4 SCP Based BCI

Slow cortical potentials are low frequency oscillations in the EEG signal and they require no external stimulus. Birbaumer et al.'s study on slow cortical potential showed that it is possible to modulate the SCPs by user training and thereby to enable the user to control objects on a computer screen[7]. 'Thought Translation Device ' was the first BCI paradigm driven by SCP control. EEG was recorded from the vertex which are referred as linked mastoids(behind the ear). Suitable filtering method was applied to extract the SCP from the EEG signal and the user was presented with a computer screen which gives a visual feedback.The feedback was in such a way that the user would be able to move a cursor on the screen by modulating the SCP signal. Selection process took 4 seconds. The system took the first 2s as baseline and measured the initial voltage level. In the next 2s, user would be able to move the cursor by self regulating the voltage level. Training sessions of 1-2 hours/week were given and they were carried on up to several months until the user achieved an accuracy of more than 75%. Once the user attained consistent performance in TTD, he/she could be shifted into language support program (LSP). LSP allowed the user to select letters or a combination of letters to form words. Users were able to achieve a selection rate of 2-36 words/hour with an accuracy of 65-90%[7]. This type of system is suitable for ALS patients when there is no communication paradigm available.

2.3.5 SMR based BCI

Sensorimotor rhythms are the μ-rhythm and β-rhythm which are oscillations occurring in the left and right sensory cortex of the brain. The attractive feature of

SMR is that it is possible to elicit SMR with motor imagery[9], making it possible for disabled subjects to use them. Hence actual movement is not needed to control the BCI. Furthermore, with training and practice, the users can modulate their SMR. Wadsworth BCI and Graz BCI are the two prominent groups concentrating on SMR based BCI research.

2.3.5.1 Wadsworth BCI based on SMR

Wolpaw, McFarland and their colleagues developed BCI systems which enabled subjects to control one dimensional or two dimensional cursor movement on a computer screen by regulating their μ and β rhythms[32, 8, 33]. In the one dimensional cursor control experiment, the user was asked to move the cursor to hit the target at the top and bottom of the monitor by regulating his/her SMR. The user increased the amplitude of 8-12 Hz μ-rhythm to move the cursor to the top of the screen and decreased the amplitude to bring the cursor to the bottom target. Regression analysis approach was used to control the cursor movement because of its suitability in multi-dimensional and continuous control. Wolpaw and McFarland demonstrated a two dimensional cursor control, based on regression approach. In the experimental trial, a target appeared among one of the eight pre-set locations on the screen. After one second, a cursor would appear at the centre of the screen and it would be able to move in two dimensions by the changes in user's EEG activity. The user was allowed to select the target location within 10s and if it happens, the target would flash in response to a successful hit. If the user fails to select the target, the target simply would disappear. This would bring the end of the trial and the screen would become blank for one second and a new target would appear again. Usually users would learn to control cursor movement in a 40 minute session over several weeks. Most of the users achieved significant cursor control during the 2-3 week training session. Initially the user performed motor actions by imagining motor activity. But by gaining experience, user would be able to control the cursor as they perform normal motor actions.

Table 2.1: Summary of control signals in BCI[13]

Signal	**Physiological Phenomenon**	**Training**	**Information Transfer Rate**
VEP	EEG variation in the visual cortex	No	60-100 bits/min
SCP	Slow voltage shift in the brain signals	Yes	5-12 bits/min
P300	Positive peaks due to rare stimulus	No	20-25 bits/min
SMR	ERD/ERS	Yes	3-35 bits/min

2.3.5.2 Graz BCI based on SMR

Graz BCI system also uses sensorimotor rhythms as control signal. This research group focuses more on motor imagery of simple motor actions (eg: imaginary hand movement) to modulate SMR and use it to control BCI systems[9]. More specifically, event related synchronization/desynchronization (ERD/ERS) during motor imagery are used as control signals. This system is a synchronous system i.e., feature extraction is performed during a predefined time window. The Graz BCI system consists of a standard experimental protocol[34]. According to this protocol, the user attends a training session to select a motor imagery paradigm. During a 5.2s window, user imagines a motor movement(eg: left or right hand, tongue, foot etc) while the features of the EEG signal is extracted using power spectral analysis. An n-dimensional feature vector is generated for each motor imagination. These vectors can be classified by a linear or non linear classifier to identify the user's motor imagination. The classifier translates the ERD/ERS into continuous output (eg: cursor control) or discrete output (eg: letter selection or word selection). Users achieved an accuracy of 90% with two choice selection by attending 6-7 sessions of training.

A summary of BCI systems based on control signals is shown in Table 2.1.

This chapter discussed about the EEG recording and common control signals employed in BCI systems. In the next chapter, different feature analysis techniques used in BCI systems will be discussed.

3 Event Detection in EEG signal

The previous chapter gave a brief introduction about various types of BCI systems and the control signals used in BCI systems. This chapter will discuss the event detection in EEG and the need for it in BCI systems.

3.1 Introduction

Almost all the current BCI systems work by extracting features from brain signals and classifying them to control external devices. Most of these features are subject specific and require specific feature extraction technique for each user. This makes the use of BCI system, laboratory oriented. Current systems are designed to extract features(eg: frequency changes) from specific locations for specific control signals. User learns to produce specific features according to the design of the BCI system. For instance, a user learns to control a cursor by imagining leg movement. When the complexity of BCI increases, the user might modulate their brain signals to make different task selection. As time progresses, the user adapts to new signals and this might cause changes in their features (eg:amplitude, frequency, location etc). Under these circumstances, it is difficult to extract information using pre-defined extraction criteria in the BCI system.

To overcome this difficulty, in 2008 Schalk et al. proposed a method that detects some changes in a set of relevant features in brain rather than detecting particular changes in specific features[35]. In their approach, they have modelled the features of EEG under rest into Gaussian mixture models and compared this model with models of EEG under other conditions. The measure of changes between two classes of EEG was used to control the BCI system rather than classifying it. The parameters of the Gaussian mixture model were estimated using EM algorithm. They have implemented this method on a real-time in a software package called SIGFRIED. The features were extracted using frequency domain approach. The number of Gaussian models was chosen experimentally.

3.2 Expectation-Maximization Algorithm

Expectation-Maximization (EM) algorithm is a method to estimate the parameters of a probability distribution. In the earlier days, parameters of complex probability distributions were estimated manually and this led to suboptimal estimation of the parameters. EM algorithm overcomes this impediment with great accuracy. This algorithm is well suited for a situation where the observed data is not complete and the algorithm estimates the parameters of the probability distribution by maximizing the likelihood function from the observed data. The concept of EM algorithm was proposed by Dempster et al. in 1977[36]. The algorithm consists of two steps: expectation and maximization. In the expectation step, the algorithm guesses the parameters of the model and computes the probability using these parameters. Maximization step utilizes the probability obtained during the expectation step and computes new parameter values. This process will continue until it reaches a convergence where no more improvisation in the probability function is possible. EM algorithm has been used in many fields such as parameter estimation, image reconstruction, finding missing data and hidden Markov model for speech recognition. Tutorial and application of EM algorithm is available in [37, 38]

3.2.1 EM algorithm in EEG

Parameter estimation of probabilistic models using EM algorithm have appeared in literatures related to brain signals. In a study by Khan et al., estimation of the ERD from the EEG signal by using a time varying auto regressive model has been described. The parameters of the model were estimated using EM algorithm. The coefficients of the model were computed using a Kalman filter[39]. Time varying spectrum of coefficients obtained from Kalman smoother was computed and its power has been calculated.[40]. The ERD was computed by comparing the obtained power with a reference value.

EM algorithm has also been used to classify single-trial ERPs elicited based on different stimulus presentations. In a recent publication, Tzovara et al. used EM algorithm to estimate the parameters of voltage topographies modelled using GMM[41]. In their study, they were able to classify VEP datasets from voltage

topographies under different stimulus presentations. The results from the single-trial ERP based on EM algorithm were compared with averaging method, the results which were found to be inferior to the former. This algorithm modelled voltage topographies using GMM for two experimental stimuli during the training phase of the algorithm.

Gaussian mixture modelling has been applied in Electrocorticogram (ECoG) also to detect epileptic seizures in the waveform. In 2004, Meng et al. developed an algorithm that modelled features of the ECoG into GMM using wavelet transform. It was a hybrid algorithm that initially decomposed the raw ECoG into sub-bands to separate seizure and no-seizure components using discrete wavelet transform. Following decomposition, a median filtering was applied to choose the envelope of the waveform. This was made into a 24 dimensional feature matrix. These features were modelled into mixture of Gaussians. Expectation-Maximization algorithm was implemented to estimate the parameters of the model. The seizure detection algorithm stored likelihood functions of both seizure and non-seizure features. A thresholding criteria was made for the likelihood-ratio and that was used to detect the beginning of the seizure events. This algorithm was able to detect seizures within 1.8s on-line[42].

All the methods discussed above used EM algorithm or variance of EM algorithm to estimate the parameters of GMM. These methods used sophisticated filtering to extract useful features from brain signals. These kinds of complicated filtering methods might cause usage of more resources and delay in processing brain signals. BCI systems require higher information transfer rate in order to work on a real-time basis. An efficient and reliable feature analysis is the key to real-time event detection. Coming sections will discuss various feature analysis technique suitable for the stated task.

3.3 Feature Analysis Techniques

A typical BCI system consists of

1. **Data Acquisition:** This is the first step of any BCI system. This stage measures EEG signal from the brain using electrodes and amplifies the EEG signals to a considerable level by a dedicated amplifier. This is followed by a

digitization step which enables the signal to be fed into a computer system for further processing. According to the control signals taken into consideration, electrode positioning may vary because different signals originate from different parts of the brain. For example, SSVEP is prominent in the visual cortex of the brain.

2. **Pre-Processing:** EEG signal is contaminated by sources like power line interference, electronic noises and electromagnetic waves. In addition to the above said noises, EEG might be disturbed by motion artefacts and other physiological signals. The data processing stage uses specific filters to clean the EEG data.

3. **Feature Extraction:** This stage of the BCI identifies the features of EEG signal. Methods used by BCIs may vary according to the control signals used. For instance, ERD/ERS requires time frequency distribution in order to see the decrease followed by an increase in the amplitude of power spectrum.

4. **Classification:** Once the feature of the signal is identified, it can be classified using appropriate algorithms. This stage actually translates the user's intention into device commands[13].

A general block diagram of BCI system is shown below. Since this study concentrates only on detecting events in the EEG data, this chapter emphasizes on different feature extraction techniques suitable for BCI system.

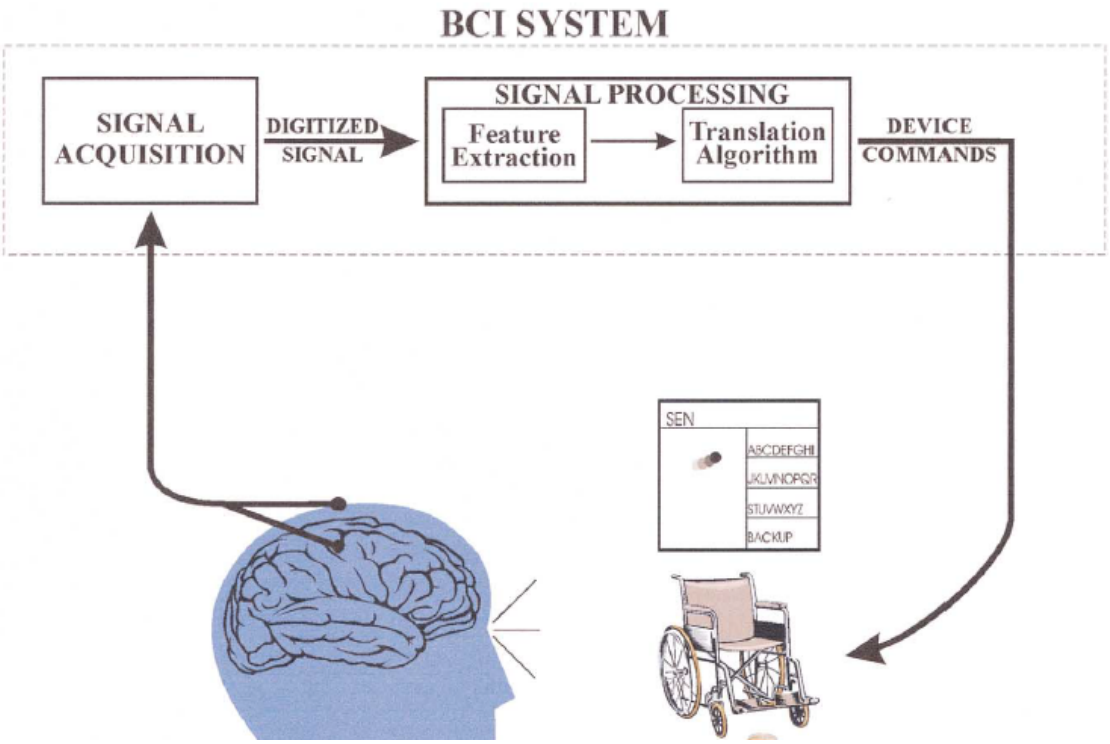

Figure 3.1: Block Diagram of BCI System. Signals from the brain are acquired using scalp electrodes and the signal processing unit extract specific features and translates them into device commands.[4]

3.4 EEG Analysis

To understand and study about different changes in the EEG signal, a good analysis technique must be used. Raw EEG does not provide much information about the ongoing activities. EEG data should be viewed in different domains to get a clear idea about the brain's activity.

3.4.1 Signal Averaging

In time domain,the traditional technique employed for detecting event related potential is signal averaging . EEG data of several experimental trials conducted with same stimulus are averaged together to get the perturbation in the signal caused by the stimulus. The time-locked variations in the EEG can be revealed using averaging

technique[43].

3.4.2 Event related spectral perturbation

In the time-frequency domain approach, the frequency power spectrum of time-locked signals are averaged together to produce event related spectral perturbation. Events can cause changes in the frequency power spectrum of the on-going EEG. ERSP is used as a visualisation tool to see mean event spectral power over a range of frequencies and time durations. ERSP of n trials is given by

$$ERSP(f,t) = \frac{1}{n}\sum_{k=1}^{n}|F_k(f,t)|^2 \tag{3.1}$$

Where, n is the number of trials and F_k is the spectral estimate of the k^{th} trial at frequency f and time t[44]. The above mentioned method is best suited for the visualisation of ERD/ERS. The output of ERSP is a 2D image that shows the power(dB) at a particular frequency and latency.

Both ERP and ERSP cannot be able to fully represent the oscillatory changes in the EEG signal. Only the time and phase locked signals would be seen in both the methods.

3.4.3 Inter-Trial Coherence(ITC)

ITC is a frequency domain analysis technique to measure the variability between time-locked single-trial EEG measurements at specific frequency and latency when EEG is measured during similar experimental events. This is referred as 'phase-locking factor' and was proposed by Tallon-Baudry et al[45]. ITC is interpreted as inter-trial phase coherence and it is arrived at by the following equation:

$$ITPC(f,t) = \frac{1}{n}\sum_{k=1}^{n}\frac{F_k(f,t)}{|F_k(f,t)|} \tag{3.2}$$

where $|F_k(f,t)|$ represents complex norm of the spectral estimate F_k and rest of the terms are same as in equation 3.1. ITC measures a value between 0 and 1 at a given significance level. Value 0 represents a poor synchronization between successive trials

and 1 represents good synchronization[44].

Study and a comparison between ERSP and ITC will give us a brief idea about the consistency of event patterns at a particular time between recorded EEG trials.

3.5 Feature Extraction

Changes occur in the pattern of the EEG rhythm due to different brain activities. These patterns have specific features which help to classify the intention of the brain. So features of the signals help to discriminate between relevant and unimportant signals. However, identifying relevant features of the brain signal is very complex. Vital information about the underlying brain process could be overlapped by multiple sources. For this reason, a simple band pass filter might not be able to extract the desired features from the brain.

The EEG signals can be analysed in time domain, frequency domain and time-frequency domain. Brain signals are transient in nature and this makes the extracting task further complicated. Tools such as Time-Frequency Analysis and Wavelet Transformation help to decompose the signal into time and frequency scale, thus enabling to see the changes in time and frequency bands.

In the coming sections, different techniques for extracting features of the EEG signals will be explained.

3.5.1 Principal Component Analysis

Most of the data recorded with high density electrodes could be redundant in nature. This results in high dimensional data and will increase the usage of computational resources. Principal component analysis is widely used to reduce the dimensions of EEG data. PCA is a statistical tool to extract features by linear transformation. PCA converts a set of correlated observations into uncorrelated variables termed as principal components. The principal components produced are sorted according to the variance in such a way that the first principal component will have the highest possible variance[13].

3.5.2 Independent Component Analysis (ICA)

ICA is a statistical technique that is used to separate mixed signals from its sources without any prior information about nature of the signal. ICA assumes that the unknown sources are mutually independent. In case of EEG signals, ICA assumes that the observed EEG is a mixture of mutually independent sources or a mixture with noises[13]. The relation between the EEG signal $x(t)$ relative to the sources $s(t)$ can be written as

$$x(t) = f(s(t)) + n(t) \tag{3.3}$$

where, f is any unknown mixture function and $n(t)$ is any random noise associated with the signal. The dimension of the vector $s(t)$ depends on the number of sources and the dimension of $x(t)$ is related to the number of measuring channels. The concept of ICA is to find the function f and to estimate the $s(t)$ by mapping the $x(t)$ on the source space. Depending upon the mixing function f, ICA can be modelled into a linear or non-linear function. However, for EEG signal, a non-linear assumption would involve inter-dimensions and hence, linear assumption is more suitable. By using the linear model equation 3.3 can be re-written as

$$x(t) = As(t) + n(t) \tag{3.4}$$

where A is the mixing matrix. $n(t)$ can be neglected by assuming the noise as zero or considering it as a negligible factor. $s(t)$ and mixing matrix A can be found by using algorithms such as Infomax. ICA can be employed to remove artifacts in EEG signals.

3.5.3 Power Spectrum

Complex signals can be decomposed into sum of sinusoidal signals with different frequencies using spectral analysis. These sinusoids can be shown in plots as magnitudes and phase between the signals. Power spectrum of the original signal is obtained by taking the power of decomposed sinusoids. Fourier Transform is a mathematical tool to decompose a waveform into sum of its sinusoidal signals. Al-

beit the frequency resolution is high for FT, its time resolution is very poor. This is due to the fact that the signal under analysis has infinite length and hence, the low resolution in time domain.

3.5.4 Time Frequency Analysis

The pitfalls in the averaging technique and ERSP could be overcome by time frequency analysis. The dynamic features of the event related potentials cannot be detected by the conventional averaging and ERSP methods. The main reason behind this is, EEG is recorded from a multiple array of electrodes and its frequency varies over time. Furthermore, the events that might be of interest could be time localized, certain information might be space localized, and sometimes restricted to specific temporalities and specific frequencies[46]. Hence, averaging and ERSP methods are not sufficient to capture the dynamic features of the event related potentials.

Short time Fourier transform (STFT) is a technique which takes Fourier Transform of the signal using a sliding window function. Since its window function is of finite duration, time and frequency information of the signal can be obtained simultaneously. However the size of the window function is fixed in STFT which limits the flexibility of this technique to analyse minute transient changes in the EEG signal.

3.5.5 Wavelet Transform

Wavelet Transform is an effective time-frequency analysis tool that uses wavelets, to manipulate non-stationary signals. Wavelets are simple oscillating amplitude functions which are localized in both time and frequency. This property is totally different from Fourier Transform, which is only localized in frequency domain and extended infinitely in time. Accurate decomposition of EEG waveforms into their component waveform is possible with Wavelet Transform. Thus isolation of functions that vary in time and space, irrespective of scale, can be achieved in WT[46]. Literatures suggest that WT offers great advantages in comparison to traditional time-frequencies like STFT with regard to component separation, signal detection and computation speed[47, 48].

Wavelets can stretch or shrink themselves and can slide through the analysed signal to capture the time and frequency information of the signal. A stretched

wavelet(large scale) is less localized in frequency and it is well suited for analysing low frequency signals. Low scaled wavelets are localized in time and are capable of extracting high frequency information from the signal. Thus, if a wavelet is localized in time, the less is its localization in frequency and vice versa. Hence, wavelets obey Heisenberg's uncertainty principle which states that there is a trade-off between time and frequency resolutions.

One of the major advantages of Wavelet Transform is that it can assume variety of shapes for the wavelets. A wavelet which closely matches with the EEG waveform can closely model the spectral and temporal characteristics of the neuroelectric signal; thereby it increases the chance of optimizing the resolution of certain events. Wavelets such as Coifman 30 or the B-Spline[46] which resemble the natural biological waveforms are suitable for EEG analysis. Raz, Dickerson and Turetsky[49] have demonstrated an improvised method for ERP decomposition from statistical estimation model by using Wavelet-Packet. This method offers precise selection of frequency and time components, even when they overlap with each other. Wavelet Transform offers design of wavelet in various shapes so that it is possible to make the wavelet template of desired shape. Hence, wavelets can precisely detect the desired events from the background EEG.

3.5.5.1 Operation of Wavelet Transform

Wavelets can breakdown the EEG waveform(or any signal) into wavelet coefficients. During the analysis, wavelets compare themselves with the signal and produce correlations called wavelet coefficients. The coefficients represent the level of the wavelet included in the analyzed signal at the given scale and time. Different scales of wavelet functions translated through the whole EEG signal produce different coefficients. Generally, whenever there is a good match in shape between the signal and the wavelet, a positive amplitude coefficient is arrived at and if the match is polarity inverted, a negative amplitude coefficient is arrived at. The original EEG signal can be reconstructed using these coefficients in the correct sequence[46].

Theoretically, wavelet analysis of EEG signals would employ infinite number of scales and time positions in order to break down the signal into small components based on the signal's time, frequency and amplitude. The result would be infinite number of wavelet coefficients. However, in practical situations, there are several

solutions available to compute the WT of the EEG signals without computing infinite coefficients. Two important methods are Continuous Wavelet Transform (CWT) and Discrete Wavelet Transform (DWT).

3.5.6 Continuous Wavelet Transform

Continuous Wavelet Transform computes coefficients of signal by scaling and translating the wavelet in small steps until it covers the whole signal. Mathematically it can be expressed as

$$c_{a,b} = \int_{-\infty}^{\infty} E(t) g *_{a,b} (t)\ dt \tag{3.5}$$

where

$$g_{a,b} = \frac{1}{\sqrt{a}} g(\frac{t-b}{a}) \tag{3.6}$$

and $*$ represents complex conjugate. Equation 3.5 shows that an infinite number of wavelet coefficient, $c_{a,b}$, is obtained by correlating any continuous signal $E(t)$ with a continuous wavelet $g_{a,b}$ at an infinite range of scales, a and infinite range of time translations, a.

$$E(t) = k \int_{-\infty}^{+\infty} \int_{0}^{+\infty} \frac{c_{a,b}}{a^2} g_{a,b}(t) da db \tag{3.7}$$

Equation 3.7 tells that the wavelets coefficients obtained from the equation 3.5 can be reconstructed to the original form.

3.5.7 Discrete Wavelet Transform

CWT produces unnecessarily high redundant coefficients due to closely spaced scales and time points. Thus CWT uses more computing resources and consumes more time to produce wavelet coefficients. Discrete Wavelet Transform is an efficient tool to compute wavelet coefficient. Unlike the CWT, that produces thousands of redundant coefficients, DWT only computes coefficient as many as there are samples in the signal analysed without causing any loss of information[46]. However, CWT is required to detect small latencies in the analysed signal.

3.5.8 Application of Wavelet Transform in EEG Signal

Hsu et al.[50] applied continuous wavelet transform to extract features of ERD/ERS to classify right and left hand motor imagery. This group constructed a 2D image of time frequency features and compared it with 2- sample t-statistics to classify the MI. The CWT allowed them to locate the event related ERD/ERS among the highly redundant wavelet coefficients. In another study, Demiralp et al., extracted P300 waveform from EEG signal using B-spline discrete wavelet in single trial analysis.[51]. P300 was elicited during an oddball paradigm.

3.6 Information Transfer Rate

The performance of a BCI system can be evaluated by measuring the number of bits (information) transferred per unit time. ITR depends on dimensionality of the control signals extracted from the raw form and accuracy of the classification of input data. ITR can be calculated depending upon the number of choices of selection per trial and if the probability of selection of choices are the same[4], ITR is calculated as follows:

$$ITR/trial = \log_2 N + P \log_2 P + (1-P) \log_2 \left[\frac{(1-P)}{(N-1)}\right] \tag{3.8}$$

where N is the number of possible choices and P is the probability of correct selection (accuracy).

Figure 3.2 shows ITR in bits per trial or bits per minute with respect to accuracy under different values of N. From the figure it is clear that with greater accuracy in selection the bit rate increases.

Better information transfer rate requires high accuracy in the classification of the data. A good feature selection technique would help to increase the classification rate and thereby to improve the ITR. This study is aimed to developing an event detection technique which is expected to improve the flexibility of BCI system.

This chapter gave an introduction about event detection in EEG signals using EM algorithm and discussed various feature analysis techniques used in EEG signals. Next chapter will discuss the experimental setup methodology of the current study.

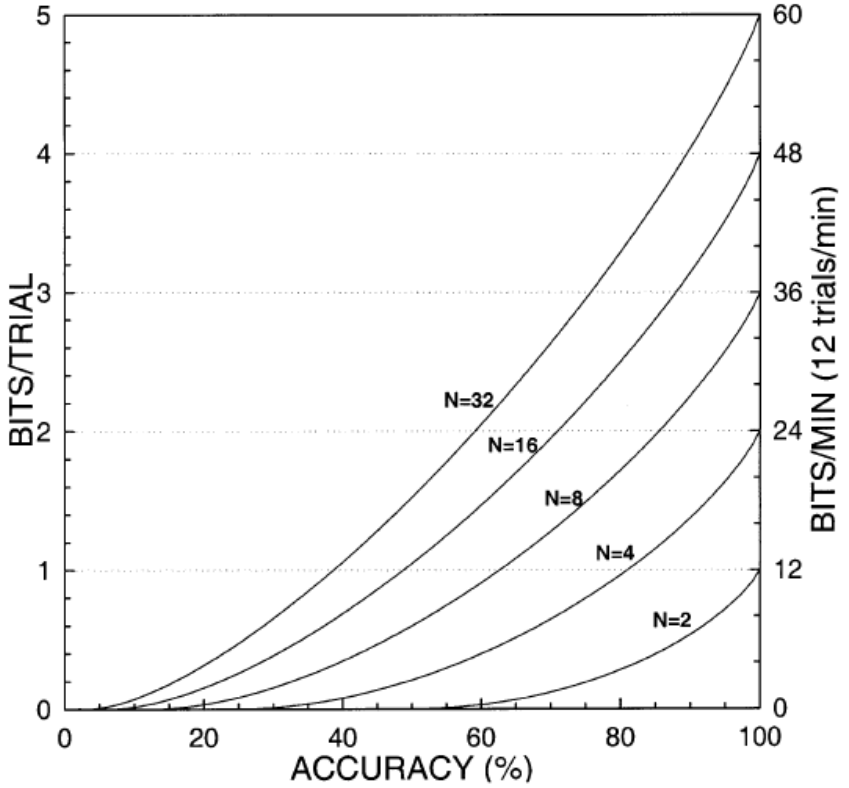

Figure 3.2: ITR in bits/trial and bits/min with different possible number of choices (N) plotted against accuracy in percentage. As the accuracy of selection increases, bits/trial or trials/min also increases. [4]

4 Methodology

Previous chapter discussed about the application of EM algorithm in EEG and various feature analysis technique available for EEG signals. This chapter will explain the experiment protocol and the process of EEG data acquisition.

This study aims at developing an algorithm to detect the intention of the user before the onset of motor action and motor imagery. Right hand wrist movement has been chosen for the analysis of motor action and motor imagery. EEG data were obtained from the experiment conducted in the Neurophysiology Lab of Strathclyde University's Biomedical Engineering department. Four normal (all Male) subjects aged between 23-26 participated in the experiment. All the subject had good vision and had no disability during the trials. The experimental procedure is explained in detail in the coming section.

4.1 Experimental Setup

Same experimental protocol was adopted for all the four subjects and the protocol adopted here closely matches the experiment conducted previously in the Neurophysiology lab of the Biomedical Engineering department[52]. The experiment required subjects to either move or imagine right hand wrist movement. Movement consisted of flexion and extension of the wrist. During the trials, the subject was asked to be seated in front of a computer screen, and was instructed to hold a manipulandum (an instrument to measure the rotation of the wrist in X and Y direction) with the right hand. The computer screen showed visual cue (boxes appeared on the right and left side of the screen) for the experiment. Subject moved the manipulandum according to the position of cue appeared on the screen. Manipulandum consists of a potentiometer that measures the movement of the wrist and generates an electrical signal. The obtained signal would move a cursor on the computer screen on a real time. See appendix for photographs of the experimental setup. Flexion causes the cursor to move left and extension moves the cursor to the right.

To begin with the trials, the subject was asked to place the cursor in a square box, at the centre of the screen. During the trials, square boxes appeared on the

left or right of the screen in a random manner. The subject was asked to move the cursor towards the squares appearing on the screen. The time difference between the cues was 5 seconds. In the mean time the subject would bring back the cursor to the initial position. Each subject was given three tasks and each task had 200 trials. The trials were performed in 2 sessions with 100 trials each. The three tasks were:

1. **Target Acquisition:**The subject captured the cue, when it appeared on the screen using the manipulandum.

2. **Ballistic Movement:** Here the subject performed a rapid point-to-point movement towards the cue. Unlike the target acquisition, the subject was not required to capture the cue here.

3. **Motor Imagery:** During motor imagery, the subject was asked to imagine the motor movements. The cursor remained in the initial position during the trials. When the cue was presented on the screen, the subject imagined the wrist movement to move the cursor to the target.

4.2 Data Recording

Recording setup consisted of EEG signal acquisition system and a control and cue presentation system. The movement of the manipulandum was synchronized with the cue presentation system.

4.2.1 Cue Presentation System

SPIKE2® software was used to present the cue in the computer screen. The software was programmed to control the sequence and appearance of the target. SPIKE2® also controls the data acquisition system for recording the wrist movement data. The movement data from the potentiometer of the manipulandum were recorded using the CED1401 data acquisition system. The module also generates the timing of the wrist movement.

CED1401 module sampled the position signals at 100Hz and this signals were used to control the cursor on the screen in real time. The SPIKE2® software reads the timing information provided by the CED1401 module and time stamps

(event marker) the onset of the movement in the EEG data via Neuroscan Synamps. SPIKE2® was programmed to produce a unique digital marker for each position of the visual cue. This information would be required to sort out the EEG trials based on the direction of wrist movement.

4.2.2 Manipulandum

Manipulandum (see appendix) is an analog joystick type device that is used to measure the movement direction of the wrist. The device consists of a grip placed on a two axis gimbal that is capable of movement in X and Y plane. The device was fitted with two highly precise servo potentiometer in order to measure the motion of the gimbal. The potentiometer was supplied with a power source. Whenever the movement occurred, resistance across the potentiometer varied and generated a signal with respect to the change in resistance. For offsetting the movement position, the measurement system had already been provided with a second set of potentiometer. To begin with the experiment, the subject held the manipulandum at the neutral position and observed the cursor's position. In case the cursor was not at the centre of the screen, it would be brought back to the proper position by offsetting the potentiometer.

4.2.3 EEG Recording

EEG recording system consisted of 64 channel electrodes, an amplifier(SynAmp^2) system and a controlling software(SCAN4.5). The electrodes were placed on the scalp according to the 10-20 international lead system. All the electrodes were attached to EasyCap before placing it on the scalp. The priority being given to the motor cortex of the brain, electrodes were densely placed in the motor cortex area. Mastoid was chosen as the reference for EEG recording. Four electrodes were used to pick up eye blinks so that it could be used to identify the contaminated EEG.

To ensure proper positioning of the electrodes, the middle line of the electrode cap was aligned to the nasion and inion. Subject's scalp was needed to be abraded in order to make a proper contact with the electrodes. A medically approved abrasive solution was applied through the openings of the electrode cap via a smooth needle tip. Once the skin was prepared, conducting gels were applied between the electrode

and the scalp to reduce the impedance level. The impedance level was monitored using the impedance tool in the SCAN4.5 software. EEG recordings were started once the impedance level reached below 5KΩ for all the electrodes.

The gain of the Synamp^2 amplifier was set to 1000 and the obtained signals were sampled at 2 KHz. These signals were passed through a bandpass filter between 0.05Hz and 500Hz in order to remove high frequency noises. The amplifier system contains an inbuilt 50Hz bandstop filter to remove the noise caused by power-line interference.

This chapter discussed the experiment protocol and EEG recording setup adopted for the current study. The coming chapter will explain the data processing and event detection algorithm.

5 Data Processing and Event Detection Algorithm

Previous chapter discussed the experiment protocol and EEG recording setup. This chapter discusses the data analysis done on the recorded EEG data and the development of event detection algorithm.

5.1 Data Processing

EEG data recorded during the experimental session was processed off-line in order to extract the information about the movement occurred during the trials. To achieve this objective, several signal processing techniques were applied. However, before applying any signal processing technique, the raw EEG data from Neuroscan had to be marked with onset time and movement direction. The sequence of operations performed on the raw EEG data are shown in Figure 5.1. The movement data were sampled by CED1401 and recorded by the SPIKE2 software. Beginning of the movement was detected manually and the timing information was marked in the movement data with the help of SPIKE2. For synchronizing the timing between raw EEG data and raw movement data, offset correction was performed. These timing details with direction data were marked in the raw EEG data. In case of motor imagery, stimulus presentation time was marked in the EEG as movement initiation time. These time stampings of motor events were used to epoch the EEG data.

5.1.1 Epoching

Time stamped EEG data were epoched using SCAN4.5. Before epoching was done on the EEG, it was made to undergo baseline correction, linear de-trending and artefact rejection. All the operations were performed in the SCAN4.5 software. Since this study is intended to detect the time of event before the motor action, the length of the epoch was limited to 2 seconds-one second before the movement and one second after the movement. During epoching SCAN4.5 sorted the epochs based on the direction of the movement. This cleaned epochs were used for further

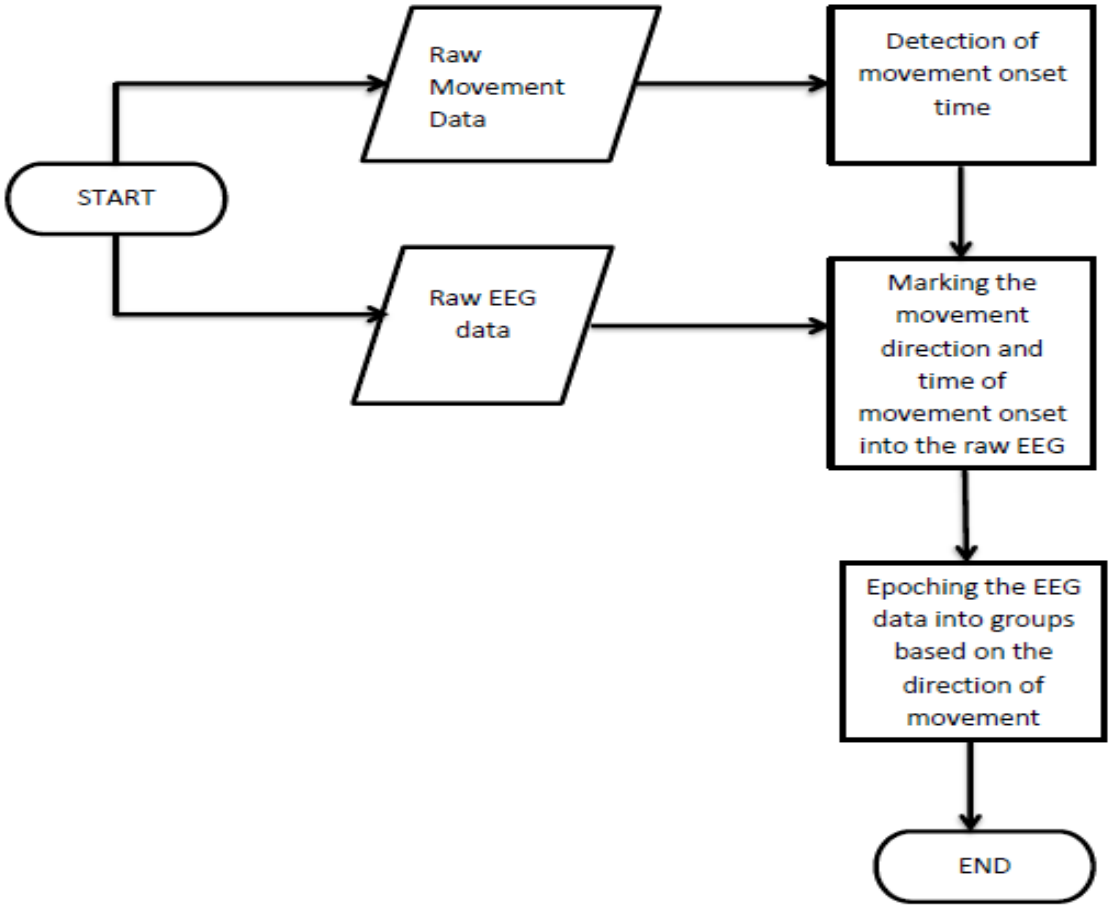

Figure 5.1: Flow chart of EEG data Processing. The process begins by marking the movement onset time into the raw EEG signal and epoching the EEG and ends by grouping the epoched data according to the direction of movement

processing.

This study, which is intended to detect motor events, takes into consideration only the C3 electrode placed in the motor cortex. Once the epoched data was ready, they were analysed in the EEGLAB[44] toolbox in Matlab for further processing. By visually inspecting the epoched data, trials contaminated with eye blinking and motion artefacts were removed. These data were re-referenced to common average by the common average referencing tool available in the EEGLAB. The common average referencing improved the signal to noise ratio.

5.2 Feature Analysis

Not all data in the epoched EEG contain relevant information about the motor activity. Moreover, it is not worth to spend computing time in analysing all the EEG data. Hence it was very important to adopt a feature selection method to suit the need of the study. This study was mainly concentrated on extracting motor events in EEG for the single trial. The following methods were employed for the same during the study.

5.2.1 Event Related Spectral Perturbation

An understanding about the changes in the power spectral distribution of EEG, during the movement was essential to develop an algorithm to detect the events. ERSP was used to study about the power spectrum in frequency domain. ERSP of all the subjects was computed using the EEGLAB. The function in the EEGLAB averages all the epochs present in the given channel. The output was a 2D image which shows the time-locked events in the EEG data. This allowed to study about the variations in the power spectrum between different subjects.

5.2.2 Inter-Trial Coherence

As mentioned in section 3.4.3, ITC was used to measure the similarity of features between single trials at a given latency and frequency. ITC was computed at a bootstrap significance level of 0.01 using EEGLAB toolbox in Matlab.

5.2.3 Wavelet Analysis

Wavelet Analysis provides the time frequency decomposition of a particular channel of the EEG data. Continuous wavelet transform was applied to the chosen channel C3 using morlet wavelet function. Morlet wavelet is a complex wavelet obtained by multiplying a complex exponential with a Gaussian window[65]. Wavelet transform was computed using the wavelet toolbox available in the Matlab. The scales for analysing various frequency bands were found out experimentally. This study was mainly interested in α-band(8-12Hz), β-band(18-24) and γ-band(28-37)

of the EEG waveform. The scales used for computing the wavelet was of the range 40-200 which covered the frequency of 5-40 Hz. The coefficients of the wavelet transform were plotted using scalogram. Scalogram computes the power of the coefficients and plots it as an image, where the colours of the image represent the percentage of power levels.

5.3 Modelling EEG Data

The study about the features in the EEG data showed that there was significant changes in the pre-movement data and post-movement data. Thus modelling the pre and post movement EEG data could serve as a standard pattern for comparison. The epoched data contains a time period of 1 second before the movement and 1 second after the movement. The first 500ms of the pre-movement were regarded as rest EEG due to the idle state of the subject. The assumption behind the algorithm was that a comparison between the rest EEG pattern and the EEG under motor task would bring some significant difference. It was expected that this difference in patterns would help to detect the events happened during motor action. The following sections will explain the modelling of the EEG data and comparison of the model with EEG under different tasks.

5.4 Gaussian Mixture Modelling

For modelling the rest EEG, a Gaussian mixture model was used. The wavelet coefficients of the EEG data were assumed to be drawn independently from a mixture of Gaussians. Let us say that the observed coefficients were $\{x1, x2, x3....x_N\}$ and they were represented as a matrix $\mathbf{N}$ of size $N \times D$ in which the n^{th} row was given by $\mathbf{x}_n^T$. Similarly, the hidden coefficients were represented as a matrix $\mathbf{Z}$ with rows $\mathbf{z}_n^T$ of size $N \times K$. In the first stage, the coefficients of wavelet were modelled into k Gaussian models and the log-likelihood function was given as

$$\ln\, p(x|\pi, \mu, \Sigma) = \sum_{n=1}^{N} \ln \left\{ \sum_{k=1}^{K} \pi_k \mathcal{N}(x_n|\mu_k, \Sigma_k) \right\} \tag{5.1}$$

where π_k, μ_k and Σ_k were mixing proportions, mean vector and covariance matrix of the k^{th} model respectively. The aim was to estimate the parameters of the model. If it was a Gaussian distribution, setting the derivative of the maximum likelihood function with respect to its parameter would give the estimate of its parameters. However, here in the case of GMM, it was a challenging task owing to the fact that putting the derivative of the MLE to zero with respect to the parameters does not give a closed-form solution. Let's come to the math part of the problem.

$$0 = -\sum_{n=1}^{N} \frac{\pi_k \mathcal{N}(\mathrm{X}_n|\mu_k, \sum_k)}{\sum_j \pi_j \mathcal{N}(\mathrm{X}_n|\mu_j, \Sigma_j)} \Sigma_k(\mathrm{X}_n - \mu_k) \tag{5.2}$$

For convenience, let's say, responsibilities

$$\gamma(z_{nk}) = \frac{\pi_k \mathcal{N}(\mathrm{X}_n|\mu_k, \sum_k)}{\sum_j \pi_j \mathcal{N}(\mathrm{X}_n|\mu_j, \Sigma_j)} \tag{5.3}$$

Equation 5.2 was obtained by setting the derivatives of $\ln p(X|\pi, \mu, \Sigma)$ with respect to μ_k. In this case, finding the μ_k was not straight forward because it requires $\gamma(z_{nk})$ to be in hand. Unfortunately, finding the probability function was unknown at this stage. Furthermore, the computation of the probability requires the parameters. Under these circumstances, the parameters could be estimated by using an expectation-maximization algorithm.

5.5 Expectation-Maximization Algorithm

Before going into the event detection of brain signals, here is given a brief introduction about the Expectation-Maximization algorithm. Following the explanation of EM algorithm, the next section will describe the application of EM algorithm in the current study of event detection.

EM algorithm is a tool to find the maximum-likelihood function of a probability distribution. The algorithm works in an iterative manner with two steps viz. expectation and maximization. The EM algorithm for Gaussian mixture modelling[53] works as follows :

1. Algorithm begins by initializing the parameters (means μ_k,covariances Σ_k and

mixing coefficients π_k) and evaluating the initial log-likelihood.

2. **Expectation Step** computes the responsibilities using the initialized parameters.

$$\gamma(z_{nk}) = \frac{\pi_k \mathcal{N}(\mathrm{X}_n|\mu_k, \sum_k)}{\sum_j \pi_j \mathcal{N}(\mathrm{X}_n|\mu_j, \Sigma_j)} \tag{5.4}$$

3. **Maximization Step** finds the parameters of the model using the responsibilities computed in the previous step.

$$\mu_k^{new} = \frac{1}{N_k} \sum_{n=1}^{N} \gamma(z_{nk}) x_n \tag{5.5}$$

$$\Sigma_k^{new} = \frac{1}{N_k} \sum_{n=1}^{N} \gamma(z_{nk})(x_n - \mu_k^{new})(x_n - \mu_k^{new})^T \tag{5.6}$$

$$\pi_k^{new} = \frac{N_k}{N} \tag{5.7}$$

where

$$N_k = \sum_{n=1}^{N} \gamma(z_{nk}). \tag{5.8}$$

4. Finally, the new log-likelihood is evaluated and the fulfilment of the convergence criterion is checked. Algorithm stops, if convergence is arrived at. Otherwise the algorithm returns to step 2.

5.6 Event Detection using EM Algorithm

The event detection technique was based on modelling the continuous wavelet coefficients of EEG into Gaussian mixture model and estimating its parameters by using EM algorithm. The log-likelihood values of coefficients between rest EEG and non-rest EEG were compared. Event would be detected, if there is any significant difference between log-likelihood values under different conditions. The detection method consisted of two phases, a training phase and a comparison phase. To detect the events, the EEG epoch(2s) was split into four equal segments. This was done to compare the log-likelihood values of each segment. The first 500ms of the epoch was considered as rest EEG. Figure 5.2 shows the segmentation of the epoch into 500ms

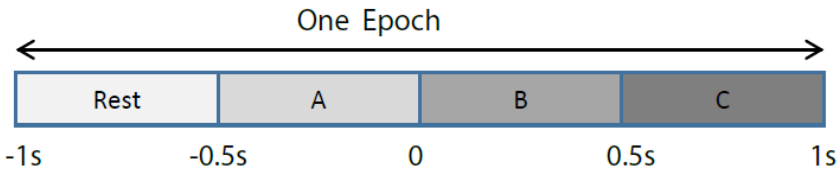

Figure 5.2: Segmentation of Epochs into 500ms windows. The onset of movement is at '0'. The first 500ms segment represents the rest EEG and A,B and C are segments of EEG with a duration 500ms each. Segment A denotes 500ms just before the movement onset, B and C denotes segments after the commencement of movement

windows. For convenience, the segments are named as 'rest', 'A','B' and 'C', where rest is the first 500ms of the epoch before the commencement of the movement, segment A denotes 500ms just before the movement onset, B is the 500ms after the onset of movement and C is the last 500ms of the epoch. These names will be used further in this thesis.

5.6.1 Training Session

This session modelled the first 500ms (rest) of the energy of the wavelet coefficients into a simple Gaussian distribution . EM algorithm estimated the log-likelihood values and these values were stored as the model log-likelihood values. Any change in the log-likelihood values of rest segments indicated the presence of events. The same procedure was done with GMM also to find whether there was any difference between simple Gaussian modelling and Gaussian mixture modelling.

5.6.2 Comparison Phase

This phase modelled the absolute power of CWT coefficient segments after the rest segment using simple Gaussian and GMM and estimated their log-likelihood values. Log-likelihood values of each segment(A,B,C) were compared with the log-likelihood estimates of the rest segment. It is expected that log-likelihood values of segments that contain features of event might be different from that of the rest segment. Hence it is possible to detect events at a particular time window.

A number of Gaussian components were experimented in both the stages. Event detection algorithm was programmed in the Matlab. As explained earlier, the core

of the proposed event detection algorithm was using EM algorithm for finding the maximum likelihood. The Matlab code for the EM algorithm was obtained from the Matlab's website[54]. The flow chart of the event detection algorithm is given in Fig 5.3.

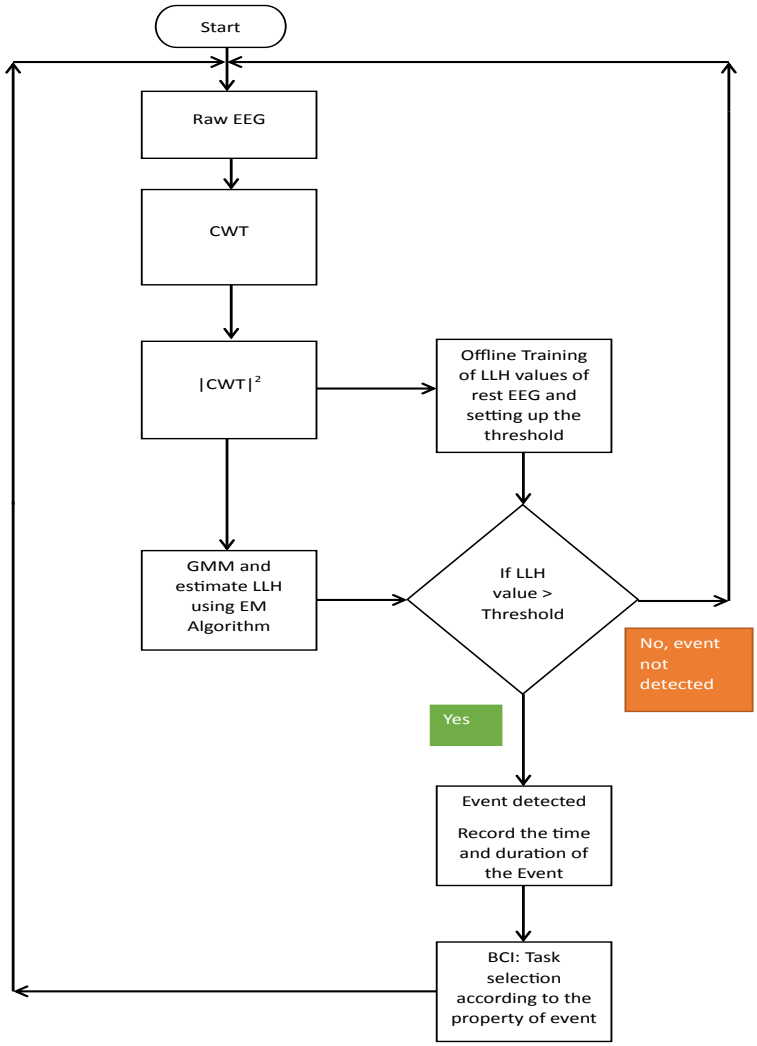

Figure 5.3: Flow chart of the proposed event detection algorithm. Algorithm begins by modelling the absolute power of wavelet coefficients into GMM of rest EEG and comparing it with the modelled EEG during motor activity. A threshold value of LLH obtained during training of rest EEG is compared with LLH values of EEG during motor action. If the threshold criteria satisfies, it would be marked as an event and proceeds for task selection. Else, the algorithm goes back to beginning step.

5.7 Statistical Analysis

The results obtained from the algorithm were statistically analysed to detect the presence of events. The objective was to find whether there is any difference existing between the mean likelihood values of two segments. Hence a A two tailed, two sample students t-test were used. This test was performed in Microsoft Excel 2010. To perform the test, the variance of the samples were assumed to be equal because the data were obtained using same procedure(EM algorithm). For samples assumed of equal variances, a pooled standard deviation was calculated using the following equation:

$$s_p = \sqrt{\frac{\sum_{i=1}^{n1}(x_{1i} - \bar{x_1})^2 + \sum_{i=1}^{n_2}(x_{2i} - \bar{x_2})^2}{n_1 + n_2 - 2}} \tag{5.9}$$

where n_1 and n_2 are the number of data in each sample, x_{1i} and x_{2i} are the corresponding individual data in each sample and $\bar{x_1}$ and $\bar{x_2}$ are the means of the two samples. The denominator of the equation represents the degrees of freedom associated with the pooled standard deviation[55].

In order to test the differences in mean, two hypotheses were proposed: null and alternate hypotheses. In all the tests null hypothesis was that there is no difference between the mean values ($H_0 : \mu_1 = \mu_2$) and the alternate hypothesis was that there are differences in mean values of the log-likelihood values ($H_a : \mu_1 \neq \mu_2$). The test statistic to judge the mean difference was given by

$$t = \frac{|\bar{x_1} - \bar{x_2}|}{s_p\sqrt{(\frac{1}{n_1} + \frac{1}{n_2})}} \tag{5.10}$$

The decision to accept the null hypothesis or to reject the alternative hypothesis depends on the comparison between the calculated t-value and the standard t-value(t_{crit}) taken from the standard Student's t-distribution at a given significance level(α). The decisions can be made upon the following conditions:

1. If $|t| > t_{crit}$, one can reject the null hypothesis and accept the alternate hypothesis.

2. If $|t| < t_{crit}$, then do not reject the null hypothesis.

It is also possible to arrive at a conclusion by looking at the P-value. Where P is 'the probability that a value of t greater than or equal to the calculated value could have occurred by chance if there were no difference in the means'[55] The next chapter will furnish the results of the current study.

6 Results

Previous chapter discussed the event data processing and event detection algorithm. This chapter will explain about the results obtained during the study.

6.1 Raw EEG data

Raw EEG data obtained during the trail is shown in figure 6.1. The data contains digital markers with the time and position information of the appearance of the visual cue(subject moved wrist according to the position of the cue). Where the markers 9 and 3 represent right and left wrist movement respectively. Disturbance in the last three electrodes(EOG1, EOG2 and EOG3) indicated eye blinks and the corresponding data were omitted from the study.

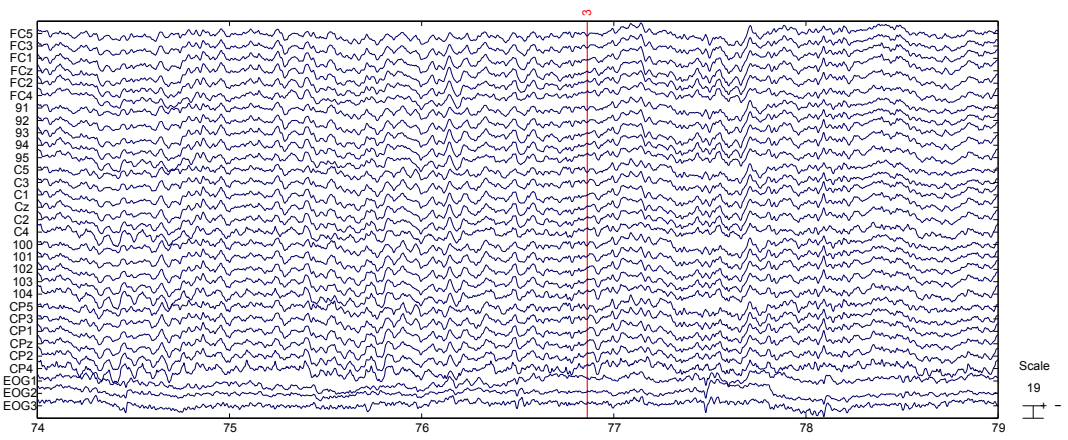

Figure 6.1: Raw EEG data with event marker 3. Event marker three represents movement towards right

6.2 Results of ERSP and ITC

This section discusses the results obtained for different experimental sessions as explained in section 4.1. Event related spectral perturbation was used to study about the prominent changes occurred in the frequency bands of EEG during the trials. ITC were computed to study about the phase-locked features of the single trial EEG during same experiments at specific latency and frequency. All the results presented here were obtained by taking the common average reference at C3 electrode. Both the ERSP and ITC were computed at a bootstrap significance level of 0.01.

6.2.1 Ballistic wrist movement

The results presented here are obtained when subjects performed ballistic wrist movement. EEG data of subject 2 comprised 66 epochs and that of subject 4 comprised 64. Upper sections of figure 6.2 and figure 6.3 show the ERSP of subject 2 and subject 4 when they performed ballistic wrist movement, towards the right side. The onset of the movement is at t=0. The color band in the figure shows the intensity of ERSP in decibels. From the figures, it is clear that an event related desynchronization happened in the α, β and γ bands, after the onset of the movement. There is clear difference between ERSPs of subject 2 and subject 4 for the same experimental task.

Images in the lower section of figure 6.2 and figure 6.3 show the inter-trial coherence of subject 2 and 4 at all frequencies during ballistic movement of the wrist. In both the figures, a significant ITC appears at the onset of the movement at briefly around 10-13 Hz and it extends to the β- band of the subject 4. Significant ITC levels indicate the phase-locked events in EEG activity between trials. In other words, ITC shows the similarity in EEG activities between single trials.

Interestingly, there is less correlation between ERSP and ITC, indicating that EEG activity between single trials are inconsistent.

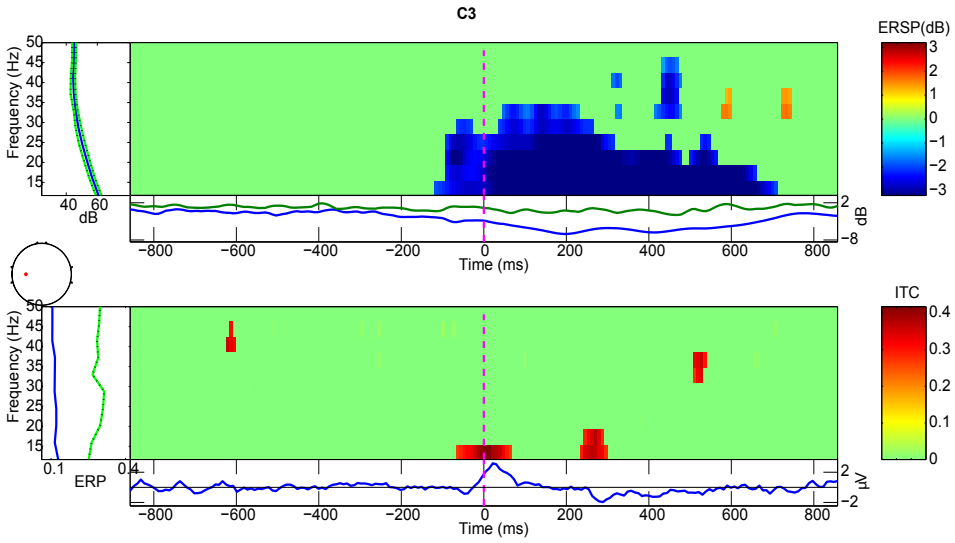

Figure 6.2: The figure shows ERSP and ITC of common average referenced EEG at C3 electrode(subject 2) when the subject performed a ballistic movement towards the right side. Image in the upper half shows the ERSP and bottom lower shows the ITC. 0 on the time axis indicates the commencement of movement.

6.2.2 Target Acquisition

Figure 6.4 and Figure 6.5 show the ERSP and ITC of subject 2 and 3 computed during the target acquisition experiment. Subject 2 consisted of 44 epochs and subject 3 consisted of 31 epochs. ERSP of the both the figure show decrease in power at the beginning of movement and it continues for 1 second post movement, around the 10-40 Hz bands of the spectrum. ITC is almost insignificant and difficult to interpret at 0.01 bootstrap significant levels. This suggests that there is high variation in phase locking between successive trials.

6.2.3 Motor Imagery

Figures 6.6 and 6.7 show the result of motor imagery when the target appeared on the left side of the screen.There were 17 epochs for subject 2 and 87 epochs for subject 4. Unlike all the previous results, ERSP (upper section of Figure 6.6) of subject 2 shows an increase in power after the presentation of the cue. This was supposed to be desynchronization instead of a synchronization. ITC for the

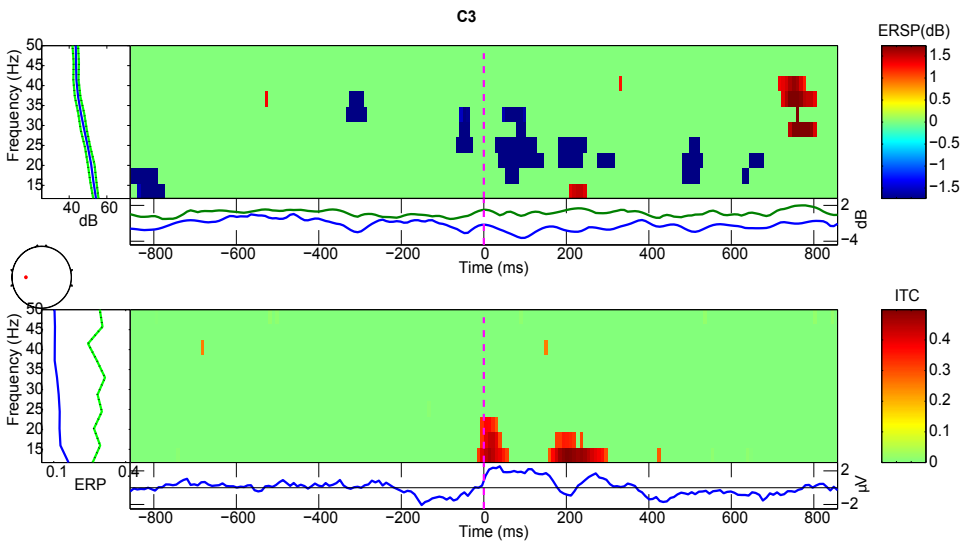

Figure 6.3: The figure shows ERSP and ITC of common average referenced EEG at C3 electrode(subject 4) when the subject performed a ballistic movement towards the right side. Image in the upper half shows the ERSP and lower half shows the ITC. 0 on the time axis indicates the commencement of movement.

same subject reveals that there is less similarity between single trials for the given experimental condition.

The upper panel of the Figure 6.7 shows the ERSP of subject 4. A slow desynchronization can be seen in the figure after the appearance of the visual cue in the α and β bands. Also some amount of increase in power can be seen around 35-45 Hz bands. There is no significant ITC in any of the frequency bands. This shows that motor imagery experiment trials were not conducted properly.

Almost all the C3 averaged ERSP for different subjects showed here, had an event related desynchronization after the appearance of the cue. This can be seen in different frequency bands viz. α, β and γ. However, ITC reveals that the events were not phase locked between successive trials.

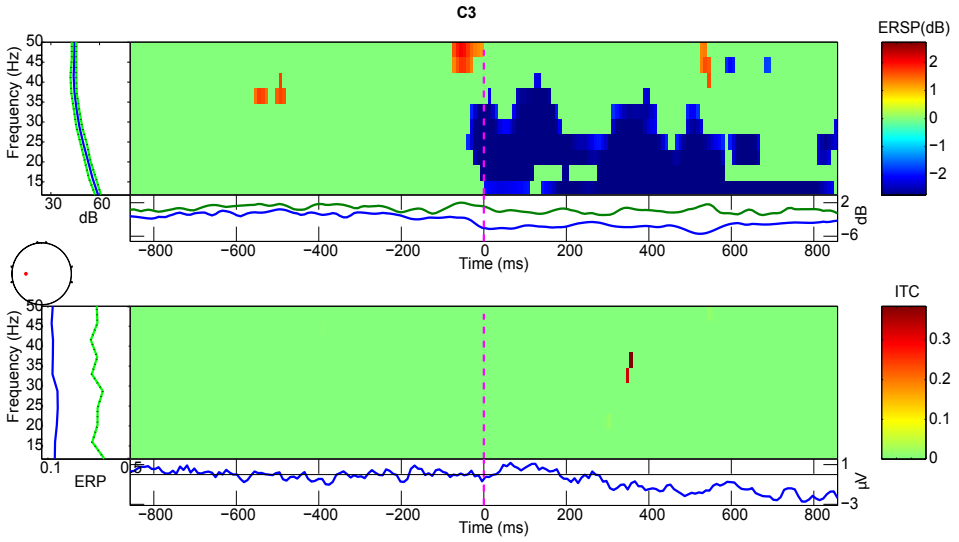

Figure 6.4: The figure ERSP and ITC of common average referenced EEG at C3 electrode (subject 2) when the subject undergone target acquisition trial towards the left side. Image in the upper half shows the ERSP and lower half shows the ITC. 0 on the time axis indicates the commencement of movement.

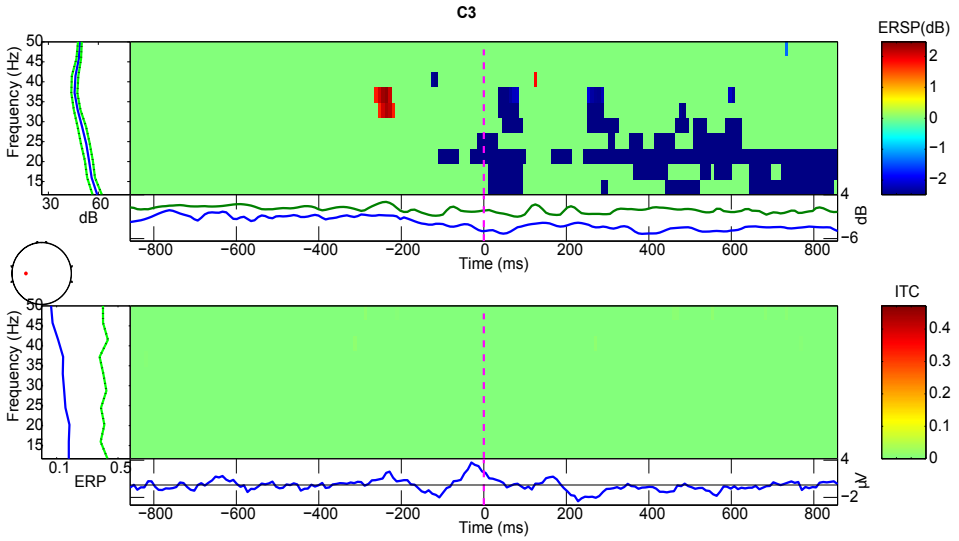

Figure 6.5: The figure shows ERSP and ITC of common average referenced EEG at C3 electrode (subject 3) when the subject undergone target acquisition trial towards the left side. Image in the upper half shows the ERSP and lower half shows the ITC. 0 on the time axis indicates the commencement of movement.

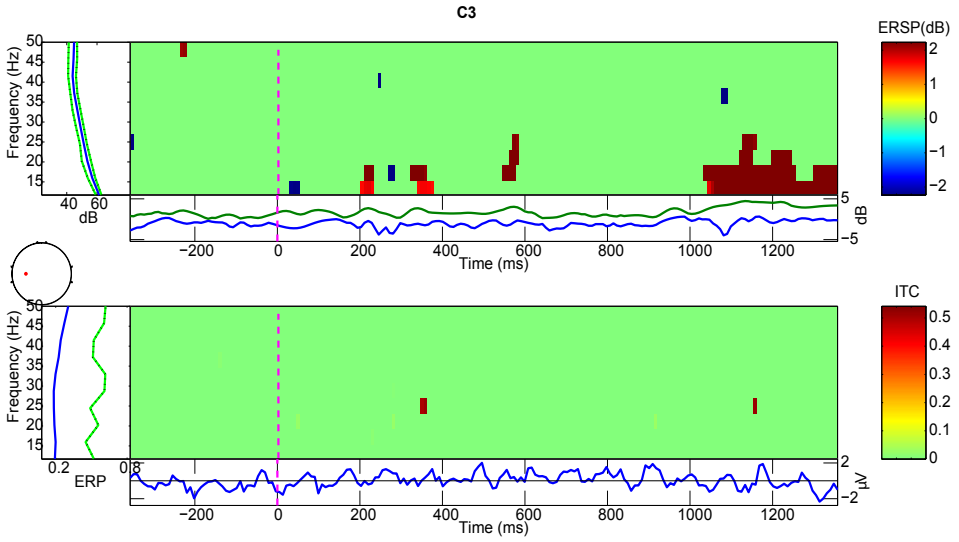

Figure 6.6: The figure shows ERSP and ITC of common average referenced EEG at C3 electrode(subject 2) when the subject imagined a wrist movement towards the right. Image in the upper half shows the ERSP and lower half shows the ITC. 0 on the time axis indicates the commencement of movement.

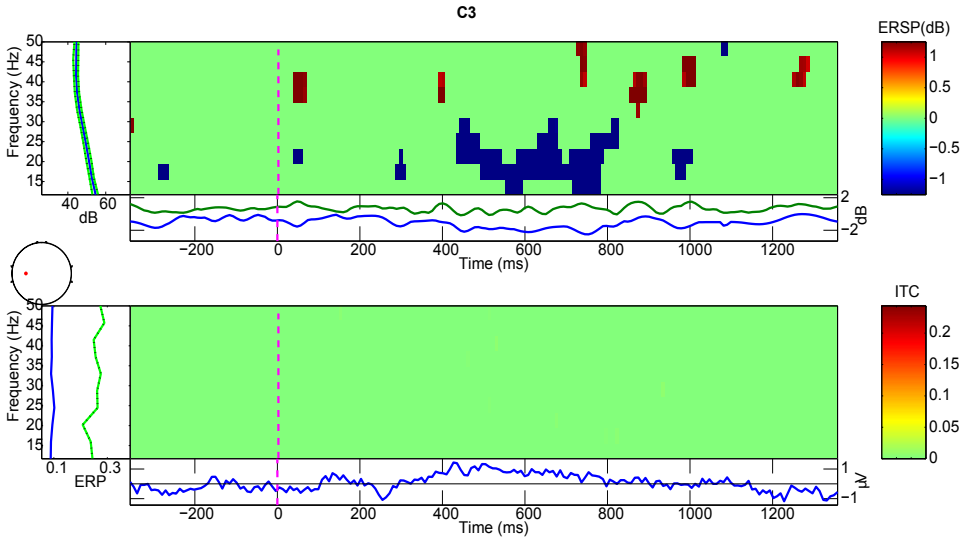

Figure 6.7: The figure shows ERSP and ITC of common average referenced EEG at C3 electrode (subject 4) when the subject imagined a wrist movement towards the right. Image in the upper half shows the ERSP and lower half shows the ITC. 0 on the time axis indicates the commencement of movement.

6.3 Continuous Wavelet Transform

Continuous wavelet transform of the common averaged C3 electrode was obtained using the process explained in section 5.2.3. The results of the CWT is presented here as scalograms. Scalogram provides information about the energy of wavelet coefficients as color maps. The vertical axis of the scalogram is converted from scale into frequency (in Hz) using the *'time2freq'* function in the Matlab. The horizontal axis stands for time in seconds. To study about the consistency of wavelet coefficient patterns between trials, average of the coefficients were calculated and its scalogram is presented here. Figure 6.8, Figure 6.9 and Figure 6.10 are the scalogram of ballistic wrist movement, target acquisition and motor imagery respectively. In all the scalograms, an event activity can be seen around the onset(t=0) of the movement(at the time of appearance of the cue, in case of motor imagery), in the α and β bands of the EEG.

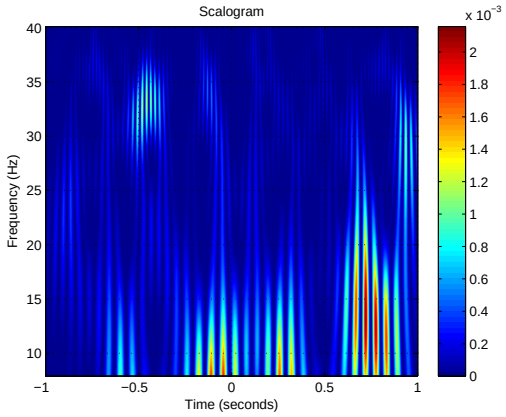

Figure 6.8: Scalogram of averaged wavelet coefficients of CAR obtained at C3 electrode across trials when subject 3 performed ballistic wrist movement (right). 0 on the time axis indicates the commencement of movement.

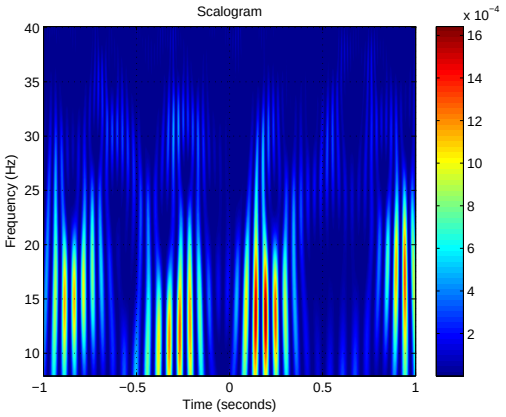

Figure 6.9: Scalogram of averaged wavelet coefficients of CAR obtained at C3 electrode across trials when subject 2 performed target acquisition (right). 0 on the time axis indicates the commencement of movement.

Event activities concentrated at the beginning of wrist movement are of interest. The results of single trial scalogram for different subjects under different experimental conditions are shown here. Figure 6.11 depicts the scalogram of ballistic movement

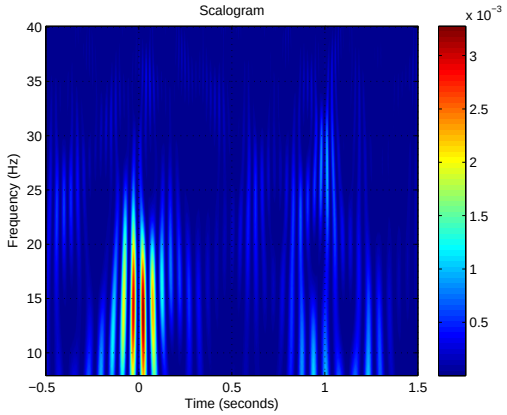

Figure 6.10: Scalogram of averaged wavelet coefficients of CAR obtained at C3 electrode across trials when the subject imagined a wrist movement towards right. 0 on the time axis indicates the commencement of movement.

of the wrist towards the left side. An event activity can be seen after the onset of the movement around the β band of the EEG data. The other two figures show that (target acquisition and motor imagery), an increased activity begins just before the movement onset in the α-band of the scalogram. To detect motor related events before the actual motor action, these features are very important. Interestingly, there is no consistency found between different trials.

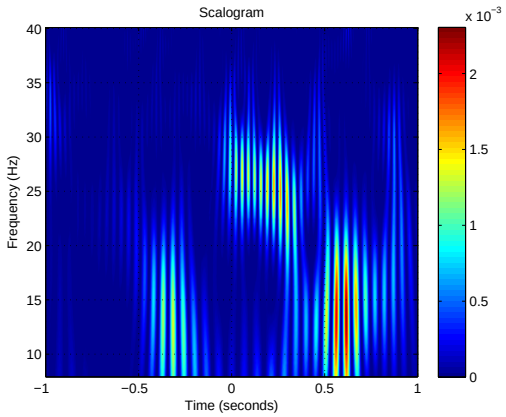

Figure 6.11: Scalogram of wavelet coefficients of CAR obtained at C3 when the subject 2 performed ballistic movement towards left side. 0 on the time axis indicates the commencement of movement.

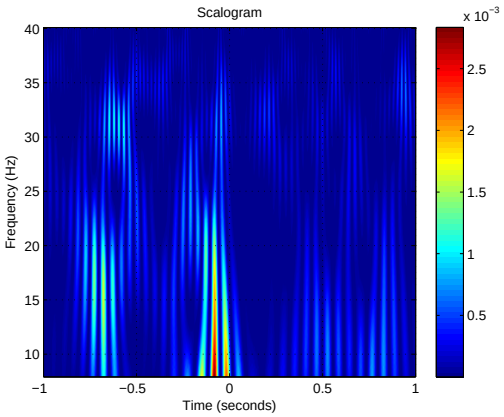

Figure 6.12: Scalogram of wavelet coefficients of CAR obtained at C3 when the subject 1 performed target acquisition towards left side. 0 on the time axis indicates the commencement of movement.

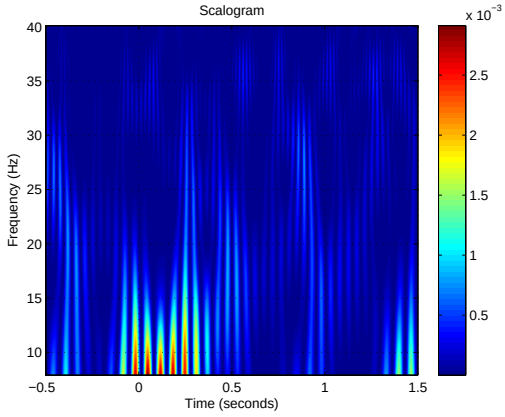

Figure 6.13: Scalogram of wavelet coefficients of CAR obtained at C3 when the subject 3 imagined a wrist movement towards right side. 0 on the time axis indicates the commencement of movement.

6.4 Results of EM Algorithm

EM Algorithm was used to model the power of wavelet coefficients into Gaussian mixtures. The input to the EM algorithm consisted of the power of wavelet coefficients and the number of Gaussians. The energy of wavelet coefficients was computed and given as an $N \times D$ matrix to the input of EM algorithm. In the current study, the number of Gaussian models has been chosen as one and two. The output of the algorithm was the parameters of the Gaussian modelling, which include component means, covariance matrix, mixing proportion and log-likelihood values. To detect the motor events, the maximum log-likelihood function was computed for the rest EEG and the EEG under motor activities. A two sided, two sample t-test was performed to compare the differences in mean of the maximum likelihood values. The results shown below are the comparisons of different subjects under different criteria.

Although this study had recorded four subjects' EEG data, only two subjects (subject-2 and 3) were chosen for the Gaussian modelling due to their better ERD results from the ERSP and ITC (see Figure 6.2 and 6.5).

6.4.1 Gaussian Distribution

The results discussed here are log-likelihood values obtained by modelling the power of continuous wavelet coefficients into a single Gaussian distribution. All the results were compared statistically by using two sample student's t-test. For comparison purpose CWT coefficients were segmented as explained in section 5.6. Log-likelihood values for the different segments of all the epochs were computed and a two sample t-test was performed. The t-test compared the means of rest segment with all other segments to see whether there is any significant difference in their means. All the tests here were conducted at a significance level of 0.05. The null hypothesis of all the test was that the mean of both the samples was zero.

Table 6.1 shows the result of t-test of subject-2 during the ballistic wrist movement. The calculated t stat is less than the critical t value and the p-value of 'rest Vs A' is greater than 0.05. Hence, there is no evidence to reject the null-hypothesis. This means that there is no significant difference between the log-likelihood value of coefficients of rest EEG and the coefficients just before the onset of the movement

('A'). However, the next two segments (B and C) show a significant difference in mean levels as the p-values are less than 0.05. This can be inferred as log-likelihood values of rest segment and the segments after the movement have relevant difference.

The t-test result of subject-2 during the target acquisition target acquisition experimental trial is shown in Table 6.2. The results show that there is a significant difference in the log-likelihood values between the rest and the final segment of the epoch (rest Vs C). The other two segments did not show any significant difference between mean values of rest. t-test result of subject-3 (Table 6.3) during target acquisition, shows no significant mean differences at any segments of the epochs when compared with the res EEG. The p-values of all the comparison is greater than 0.05 hence, there is no significant evidence to reject the null hypothesis.

Table 6.1: Two sided two Sample t-Test for subject 2 (Ballistic Movement). This table shows the result of statistical comparison mean LLH values (Gaussian distribution) of rest segment with segments A,B and C.

Subject 2	**Rest Vs A**	**Rest Vs B**	**Rest Vs C**
Observations	67	67	67
t Stat	0.00432	3.611	2.99
t critical two tail	1.98	1.98	1.98
p-value	0.997	0.000433	0.00324

Table 6.2: Two sided two Sample t-Test for subject 2 (Target Acquisition). This table shows the result of statistical comparison of mean LLH values (Gaussian distribution) of rest segment with segments A,B and C.

Subject 2	**Rest Vs A**	**Rest Vs B**	**Rest Vs C**
Observations	41	41	41
t Stat	0.0092	0.81	2.467
t critical two tail	1.99	1.99	1.99
p-value	0.99	0.4214	0.016

Table 6.3: Two sided two Sample t-Test for subject 3 (Target Acquisition). This table shows the result of statistical comparison of mean LLH values (Gaussian distribution) of rest segment with segments A,B and C.

Subject 3	**Rest Vs A**	**Rest Vs B**	**Rest Vs C**
Observations	31	31	31
t Stat	0.209	1.006	0.3165
t critical two tail	1.99	1.99	1.99
p-value	0.84	0.319	0.753

6.4.2 Two mixture Gaussian model

This section discusses the results of CWT modelled into two mixture of Gaussian using EM algorithm. The same subjects and experimental conditions were chosen as in the previous section, to compare any significant differences between the means of rest and other segments of the epoch. The same trend of p-values of the Gaussian distribution followed here also. Subject-2 during the ballistic movement trial shows significant differences in mean values of the segments between rest segment as in the single model Gaussian (see Table 6.4. In fact, the p-values are significantly reduced from the Gaussian distribution. In case of target acquisition trial, only the 'rest Vs C' shows significant differences in mean values (Table 6.5. This trend is same as the single Gaussian model, however, the p-values has significantly reduced. This is also same for the subject-3 during target acquisition as well (Table 6.6).

Gaussian mixture modelling with two Gaussians produced better statistical results than modelling the wavelet coefficients of EEG data with simple Gaussian distribution.

Table 6.4: Two sided two Sample t-Test when subject 2 performed ballistic wrist movement. This table shows the result of statistical comparison of mean LLH values (2 model GMM) of rest segment with segments A,B and C.

Subject 2	**Rest Vs A**	**Rest Vs B**	**Rest Vs C**
Observations	67	67	67
t Stat	0.077	4.073	3.140
t critical two tail	1.98	1.98	1.98
p-value	0.939	0.000	0.001

Table 6.5: Two sided two Sample t-Test when subject 2 performed target acquisition. This table shows the result of statistical comparison of mean LLH values (2 model GMM) of rest segment with segments A,B and C.

Subject 2	**Rest Vs A**	**Rest Vs B**	**Rest Vs C**
Observations	41	41	41
t Stat	0.015	0.997	2.997
t critical two tail	1.99	1.99	1.99
p-value	0.988	0.322	0.004

Table 6.6: Two sided two Sample t-Test when subject 3 performed target acquisition. This table shows the result of statistical comparison of mean LLH values (2 model GMM) of rest segment with segments A,B and C.

Subject 3	**Rest Vs A**	**Rest Vs B**	**Rest Vs C**
Observations	31	31	31
t Stat	0.671	1.55	0.46
t critical two tail	1.99	1.99	1.99
p-value	0.505	0.123	0.65

6.5 Processing Time

The main aim of this study was to find out the practicality of the event detection technique to be used in real-time scenarios. Processing time of the algorithm is a very important factor for the on-line use. The processing time of the algorithm was directly related to the number of scales in the wavelet coefficients and the number of models in the GMM. From this study it was observed that the algorithm took more iterations to converge in two model GMM than in the single Gaussian distribution. To use this algorithm in real-time, the dimensionality of the data should be reduced as much as possible, in order to attain a faster response to detect the events. The EM-algorithm converged all the times within 500 iterations in two model GMM. In the case of Gaussian distribution, the maximum number of iteration was two times.

This chapter discussed the results obtained during the study. The next chapter will discuss the results obtained during this study and also concludes the findings of this study.

7 Discussion

There is not much research has been done on event detection in EEG signal for BCI[56, 35]. Finding the exact time and location of an event in EEG is indeed a challenging task. The present study has investigated the application of EM algorithm in EEG signals to detect events during motor actions (ERD/ERS). Initial results show that there is some statistical difference between the log-likelihood values of rest EEG and EEG undergoing motor actions. However, more investigations and experiments are needed to validate the claim. The aim of the project was to develop an algorithm to detect events happening in the brain signals during motor actions, by modelling the features of time-frequency domain of motor activities. Previous study utilized frequency domain features to model the EEG[35]. The current study used wavelet transform to extract the features from EEG.

Flexion and extension of the wrist were chosen as motor activities for the study. Many literatures have reported that when the body prepares for a motor action or during a motor activity, event related desynchronization occurs[57, 24, 58, 59]. ERD represents a decrease in power of the α, β and γ bands of the EEG signals. Similarly, after the movement, event related synchronization occurs and this signifies an increase in power of the particular frequency bands due to the synchronization of the firing of cortical neurons. Experimental studies have shown that these events will be present during the motor imagery also.

Current study used 64 channels to record the EEG data from the scalp. Common averaged C3 electrode was chosen for the event detection study. Common average referencing was performed to reduce the influence of other electrode sources surrounding the C3 electrode. This in fact helped to reduce the noise levels when compared to the normal referencing.

7.1 Data Processing

The aim of the study, which has been mentioned above, has influenced the length of the epoch. For motor experiments, the duration of the epoch was 2s-this included 1s pre-movement and 1s post-movement-and in case of motor imagery, 0.5s before

the movement and 1.5s after the commencement of the movement. The objective was to detect the intention of the user before the actual motor action. It has been reported in literatures that whenever a person is about to perform a motor action, our brain prepares for the movement by an increasing activity in the motor area. This phenomenon has been termed as Bereitschaft potential or readiness potential[60]. For motor imagery, 1.5s window was allocated post movement because it is hard to know when the subject actually imagine the movement.

7.2 ERSP

Event related spectral perturbation gave an insight about the changes occurring in the frequency spectrum of the EEG during motor activity and motor imagery. Event related desynchronization was visible in the α, β and γ bands of the EEG signal, irrespective of the experimental conditions. It was evident that the decline of power has started just before the onset of the movement and it continued till 800ms post movement (see Fig 6.2). This phenomenon signifies the existence of Bereitschaft potential. The ERD obtained using ERSP are consistent with the literatures related to ERD/ERS[61, 62]. In this study ERS was not visible due to the inadequate duration of post-stimulus EEG epoch.

In the current study, ERSP of motor imagery was not evenly seen among the subjects. One reason might be the lack of training. Moreover, the motor imagery trials were conducted as the last session of the experiments following by the target acquisition and ballistic movement trials. And as a result of a long tiresome session of experiments, concentration level of the subject might have gone down.

7.3 Inter-Trial Coherence

Inter-Trial Coherence was chosen for the study to learn about the consistency of single trials in an experimental session. ITC shows the similarities in synchronization of events in successive trials at a particular latency and frequency bands. Unfortunately, this study could not find significant ITC in the subjects, especially in case of motor imagery. This results indicate that the motor events in the epoched EEG is not consistent among single trials.

7.4 Continuous wavelet transform

Continuous wavelet transform was employed due to its high efficiency in extracting transient activity in signals. Developing an algorithm which can be employed for on-line event detection requires exact capture of event occurred at a particular time. In this study, scalogram showed the percentage of energy of wavelet coefficients of analysed signal in the range of 8-40 Hz. The average of the epoch was calculated to see the prominent activities in the EEG during different experiment taken place under different conditions. Scalogram of averaged epochs show that there are differences between activities among different experimental conditions. Much of the events are concentrated around the commencement of the movement around the α and β bands. Scalogram computed the absolute power of the continuous wavelet coefficients. Calculation of the power is by taking the absolute value and squaring the coefficients, helped to increase the difference between low correlated wavelet coefficients to highly correlated wavelet coefficients. The wavelet transform used in the current study is similar to the one used by Zygierewicz et al to extract ERD/ERS using morlet wavelet[63]. In their study, they translated the obtained coefficients into time-frequency scale and plotted the scalogram with the significant values relating to ERD. In this study this was not necessary because this study modelled the pattern of rest EEG template to detect events related to motor task.

The results of single trial EEG show that there is no similarity between trials. This goes along with the results obtained from inter trial coherence.

7.5 Event Detection Algorithm

The core of the event detection algorithm was the probabilistic modelling (GMM) of the wavelet coefficients of the EEG. EM algorithm was implemented to estimate the parameters of the model and to maximize the log-likelihood values using the estimated parameters. The algorithm works by comparing the parameters of the rest EEG with EEG under motor task. Any difference between the models could be called as an event. The proposed event detection algorithm initially creates a database of the log-likelihood values of the features (using CWT) of rest EEG and compares it with the log-likelihood values of EEG during motor activity. The

template of rest EEG was obtained by taking the first 500ms of the epoched EEG data. It was hypothesized that during the initial part of the EEG the subjects were sitting idle and hence, the first 500ms of the EEG was selected as rest EEG. Moreover, for comparison purposes wavelet transform of the single epoch EEG was divided into 500ms windows.

Initially, the wavelet coefficients were modelled into a simple Gaussian distribution and the parameters for comparison purposes were estimated. Statistical analysis of the log-likelihood values between rest EEG and EEG under motor action was accomplished by performing a two tailed, two sample student t-test. Primary results show that there have been some differences in the mean of the log-likelihood values between EEG under rest and EEG under under motor action. At a significance level of 0.05, only one subject in this study showed significant differences between rest segment of the epoch and segments after the movement. Using the current algorithm and given EEG dataset, it was unable to detect the motor event before commencement of the movement. The Gaussian model was insensitive in the current study to detect Bereitschaft potential. This might be due to inconsistency of the features of the EEG dataset. Moreover, the number of subjects was not sufficient to conclude the findings.

A Gaussian mixture modelling with two Gaussians were implemented to increase the sensitivity of the simple Gaussian distribution. This was tried with the same subjects and the results were the same. Interestingly, during the two sample t-test, the p-value has decreased further than the p-value obtained when modelled with normal Gaussian distribution. This indicates that Gaussian mixture models offer more sensitivity than a simple Gaussian distribution to elicit differences between two conditions. Albeit GMM offers more flexibility, it takes increased number of iterations to converge than the simple Gaussian distribution. Hence, as the number of Gaussians increases, the algorithm takes more time to converge at the maximum log-likelihood value.

The current study is similar to the seizure detection from ECoG based on Gaussian mixture modelling proposed by Meng et al[42]. They decomposed the ECoG signal into sub-bands and modelled the GMM using EM algorithm. Although it was an on-line detection, the algorithm took 1.8s to detect a seizure. This time delay is not favourable for BCI systems. At this stage, it is not possible to comment on the

speed of detection of the current algorithm.

7.6 EM-Algorithm

The algorithm was very robust and the integrity of the algorithm was tested by modelling a randomly generated data from a bivariate Gaussian distribution. The EM algorithm estimated the exact mean and covariance values of the generated bivariate Gaussian distribution. In the current study, in all cases of simple Gaussian distribution, the algorithm converged in two iterations. However, when the CWT coefficients were modelled using Gaussian mixture model, the algorithm took more than 2 iterations to converge. The convergence of EM algorithm depends on the initial guess of the parameters (mean and covariance). The EM algorithm used for the current study has initialized the parameters randomly. Sometimes random initializations might trap the algorithm in local maxima before attaining the true maximum log-likelihood values[64]. In the current algorithm, maximum number of iteration was set to be 500. In some cases it reached 500 iterations and gave the parameters of the 500th value as the final values of the parameters. This is highly unacceptable for the EEG event detection. These kind of values mislead the event detection algorithm and might end up with detection of false events. These could be solved by multiple random initialization of the parameters and taking the highest maximum likelihood value as the best one. However, on-line event detection technique needs to be very responsive in order to achieve its objective. Further studies should experiment the usage of other initialization techniques like k-means clustering algorithms instead of random initialization.

The number of Gaussians for the GMM was two. The result obtained shows that GMM gave much more promising result than the simple Gaussian distribution. At the present stage, it is impossible to say how many Gaussians will provide the optimum output for the event detection in EEG signals. Further experimentation with increased number of models are required to find the optimum results.

7.7 Limitations of the current study

One of the limitations of the study was the low quality of the epoched data. The results of the ITC show that there is less similarity in the patterns of events between successive trials. It might be due to these shortcomings that the results of the statistical analysis were not satisfactory. Another limitation was the less number of subjects used in the current study. To generalize the properties of current event detection algorithm, more number of subjects are needed to create a model for rest EEG template.

Like any pattern recognition or supervised learning systems, dimensionality was a problem for the current study. During the wavelet transform, the number of scales used has influenced the dimension of input to the EM algorithm. As the number of scales increased, dimension of the wavelet coefficients matrix also increased. Increased dimension of the input matrix slowed down the convergence of the EM algorithm. Moreover, initialization of the parameters would be more easier with less dimensional matrix. Due to the lack of quality in the obtained EEG epochs, this study did not try to extract specific features in EEG. By experimenting with consistent single trials, it is possible to find repeating patterns in any of the frequency bands in the EEG signals. Thereby, the dimension of the input matrix can be greatly reduced and ultimately, the speed of the convergence of the EM algorithm can be increased.

Another difficulty occurred during the time of EEG recording. Most of the subjects felt sleepy during the trials due to longer recording sessions. As said earlier in the previous section, motor imagery was conducted as the last session of experimental trials. This might have influenced the quality of motor imagery.

The following chapter concludes the thesis and discusses the future prospects of the current study.

8 Conclusion

The aim of the study was to develop an event detection algorithm for EEG signals that could be used for BCIs. The current study developed a protocol for the event detection algorithm by using a simple Gaussian distribution and a Gaussian mixture modelling. The parameter estimation of the models was done using Expectation-Maximisation algorithm. A Continuous Wavelet Transform was used to decompose the signal in time-frequency domain and it was modelled into Gaussian models. The log-likelihood values of the model of the rest EEG was compared with the models of EEG during motor task. Simple Gaussian modelling showed significant differences between log-likelihood values of rest EEG and EEG segments after the movement. GMM with two Gaussians obtained more convincing results than those of simple Gaussian distribution. More experimentations are required to find the optimum number of Gaussian models that would give better speed and reliable event detection. Even though there are limitation for the current study, the primary results look promising.

8.1 Future Works

Future works should be extracting features from any of the three frequency bands (α, β or γ) that is consistent with motor tasks thereby reducing the number of dimensions in the data. In future, this study can be extended further for real-time event detection in EEG signals. Since this study models rest EEG as a template for event detection, it can be possible to use multiple controls signal for BCI system rather than a single control signal. Moreover, there would be no need to know the exact features of the events. This would improve the classification rate and flexibility of the BCI systems.

Appendices

Experimental Setup

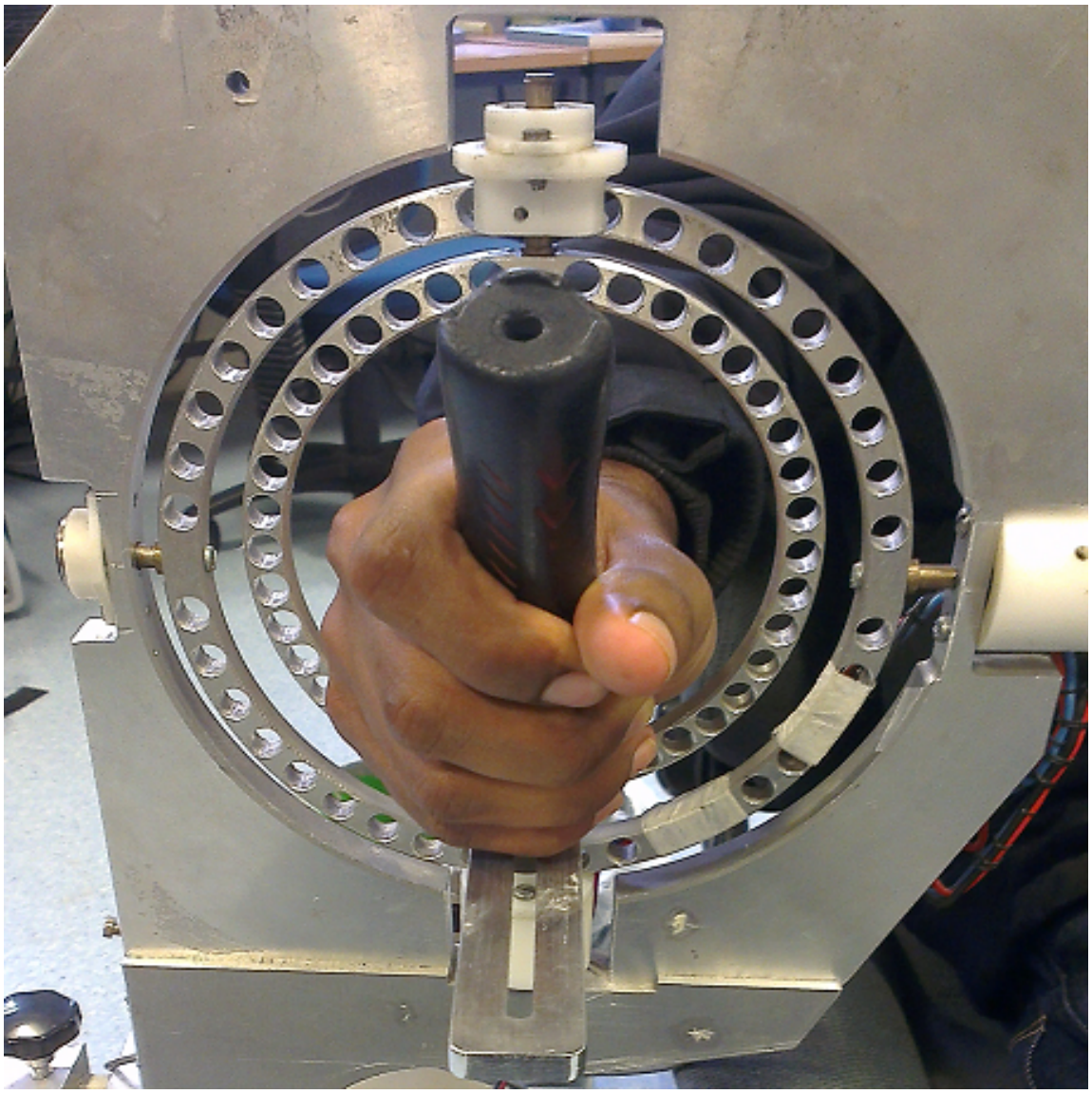

Figure 8.1: This figure shows a subject holding manipulandum. Manipulandum controls the cursor movement on the computer screen and it records the direction of movement.

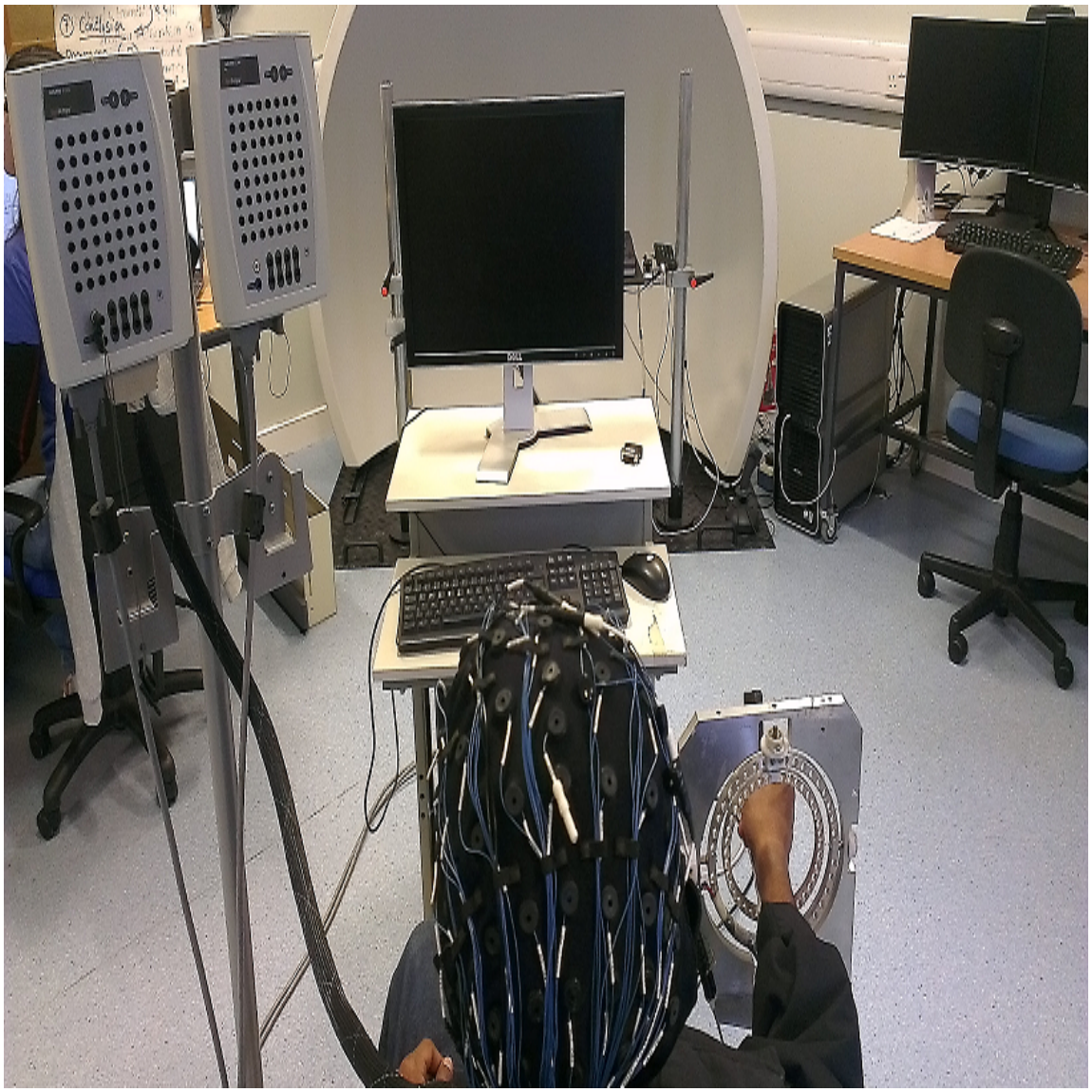

Figure 8.2: Experimental setup. This figure shows the experimental setup of the current study. In this figure, subject with electrodes placed in the scalp moving the manipulandum according to the visual cue on the screen.

Results

Statistical analysis

Table 8.1: Two sided two Sample t-Test when subject 1 performed ballistic wrist movement towards right side. This table shows the result of statistical comparison mean LLH values (Gaussian distribution) of rest segment with segments A,B and C.

Subject 1	**Rest Vs A**	**Rest Vs B**	**Rest Vs C**
Observations	4	4	4
t Stat	0.776	4.73	2.27
t critical two tail	2.45	2.45	2.45
p-value	0.47	0.003	0.064

Table 8.2: Two sided two Sample t-Test when subject 3 performed a ballistic wrist movement towards right side. This table shows the result of statistical comparison mean LLH values (Gaussian distribution) of rest segment with segments A,B and C.

Subject 3	**Rest Vs A**	**Rest Vs B**	**Rest Vs C**
Observations	62	62	62
t Stat	0.542	1.857	3.698
t critical two tail	1.980	1.980	1.980
p-value	0.589	0.066	0.000

Table 8.3: Two sided two Sample t-Test when subject 1 performed ballistic wrist movement towards right side. This table shows the result of statistical comparison of mean LLH values (2 model GMM) of rest segment with segments A,B and C.

Subject 1	**Rest Vs A**	**Rest Vs B**	**Rest Vs C**
Observations	4	4	4
t Stat	1.561	4.128	3.549
t critical two tail	2.447	2.447	2.447
p-value	0.169	0.006	0.012

Table 8.4: Two sided two Sample t-Test when subject 3 performed ballistic wrist movement towards right side. This table shows the result of statistical comparison of mean LLH values (2 model GMM) of rest segment with segments A,B and C.

Subject 3	**Rest Vs A**	**Rest Vs B**	**Rest Vs C**
Observations	62	62	62
t Stat	0.494	1.891	3.990
t critical two tail	1.980	1.980	1.980
p-value	0.621	0.061	0.000

Matlab Scripts

Scalogram

```
t = linspace(-1,1,4001);
coefs=cwt(x,40:200,'morl'); %x is the input vector
sca=wscalogram('[]',coefs);
sclf=scal2frq(40:200,'morl',1/2000);
imagesc(t,linspace(40,8,length(sclf)),sca);
shading flat;
xlabel('Time (seconds)')
```

```
ylabel('Frequency (Hz)')
title('Scalogram')
colorbar
grid
set(gca,'Ydir','normal')
```

Gaussian Modelling

```
% This script calculate the log-likelihood values of the EEG ...
    epochs for different segments
% NB: This script require EEGLAB toolbox installed in the Matlab
[m1 n1 p1]=size(EEG.data);
eegdat=EEG.data(:,:);
[m n]=size(eegdat);
%M=cell(1,p1);
MLL=zeros(p1,2);
for i=1:p1
    if i==1
%wavelet transform
wt=eegdat(:,1:1000);
coefs=cwt(wt,40:200,'morl');
sca=wscalogram('[]',coefs);
%Gaussian modelling using EM algorithm
[¬,¬,llh]=emgm(sca,2);
MLL=llh;
r=4000; % This value should be changed to select the segments
    else
        wt=eegdat(:,r:r+1000);
        coefs=cwt(wt,40:200,'morl');
        sca=wscalogram('[]',coefs);
        [label,model,llh]=emgm(sca,2);
        r=r+4000;
        maxi=max(llh);
        MLL(i,:)=maxi;
    end
end
disp('    LLH    ')
```

```
disp(MLL(:,1))
```

EM Algorithm

```
function [label, model, llh] = emgm(X, init)
% Perform EM algorithm for fitting the Gaussian mixture model.
%   X: d x n data matrix
%   init: k (1 x 1) or label (1 x n, 1≤label(i)≤k) or center (d ...
    x k)
% Written by Michael Chen (sth4nth@gmail.com).
%% initialization
fprintf('EM for Gaussian mixture: running ... \n');
R = initialization(X,init);
[¬,label(1,:)] = max(R,[],2);
R = R(:,unique(label));

tol = 1e-10;
maxiter = 500;
llh = -inf(1,maxiter);
converged = false;
t = 1;
while ¬converged && t < maxiter
    t = t+1;
    model = maximization(X,R);
    [R, llh(t)] = expectation(X,model);

    [¬,label(:)] = max(R,[],2);
    u = unique(label);   % non-empty components
    if size(R,2) ≠ size(u,2)
        R = R(:,u);   % remove empty components
    else
        converged = llh(t)-llh(t-1) < tol*abs(llh(t));
    end

end
llh = llh(2:t);
if converged
```

```
33      fprintf('Converged in %d steps.\n',t-1);
34  else
35      fprintf('Not converged in %d steps.\n',maxiter);
36  end
37
38  function R = initialization(X, init)
39  [d,n] = size(X);
40  if isstruct(init)  % initialize with a model
41      R  = expectation(X,init);
42  elseif length(init) == 1  % random initialization
43      k = init;
44      idx = randsample(n,k);
45      m = X(:,idx);
46      [~,label] = max(bsxfun(@minus,m'*X,dot(m,m,1)'/2),[],1);
47      [u,~,label] = unique(label);
48      while k ~= length(u)
49          idx = randsample(n,k);
50          m = X(:,idx);
51          [~,label] = max(bsxfun(@minus,m'*X,dot(m,m,1)'/2),[],1);
52          [u,~,label] = unique(label);
53      end
54      R = full(sparse(1:n,label,1,n,k,n));
55  elseif size(init,1) == 1 && size(init,2) == n  % initialize with ...
        labels
56      label = init;
57      k = max(label);
58      R = full(sparse(1:n,label,1,n,k,n));
59  elseif size(init,1) == d  %initialize with only centers
60      k = size(init,2);
61      m = init;
62      [~,label] = max(bsxfun(@minus,m'*X,dot(m,m,1)'/2),[],1);
63      R = full(sparse(1:n,label,1,n,k,n));
64  else
65      error('ERROR: init is not valid.');
66  end
67
68  function [R, llh] = expectation(X, model)
69  mu = model.mu;
70  Sigma = model.Sigma;
71  w = model.weight;
```

```
72
73  n = size(X,2);
74  k = size(mu,2);
75  logRho = zeros(n,k);
76
77  for i = 1:k
78      logRho(:,i) = loggausspdf(X,mu(:,i),Sigma(:,:,i));
79  end
80  logRho = bsxfun(@plus,logRho,log(w));
81  T = logsumexp(logRho,2);
82  llh = sum(T)/n; % loglikelihood
83  logR = bsxfun(@minus,logRho,T);
84  R = exp(logR);
85
86
87  function model = maximization(X, R)
88  [d,n] = size(X);
89  k = size(R,2);
90
91  nk = sum(R,1);
92  w = nk/n;
93  mu = bsxfun(@times, X*R, 1./nk);
94
95  Sigma = zeros(d,d,k);
96  sqrtR = sqrt(R);
97  for i = 1:k
98      Xo = bsxfun(@minus,X,mu(:,i));
99      Xo = bsxfun(@times,Xo,sqrtR(:,i)');
100     Sigma(:,:,i) = Xo*Xo'/nk(i);
101     Sigma(:,:,i) = Sigma(:,:,i)+eye(d)*(1e-6); % add a prior for ...
            numerical stability
102 end
103
104 model.mu = mu;
105 model.Sigma = Sigma;
106 model.weight = w;
107
108 function y = loggausspdf(X, mu, Sigma)
109 d = size(X,1);
110 X = bsxfun(@minus,X,mu);
```

```
111 [U,p]= chol(Sigma);
112 if p ≠ 0
113     error('ERROR: Sigma is not PD.');
114 end
115 Q = U'\X;
116 q = dot(Q,Q,1);  % quadratic term (M distance)
117 c = d*log(2*pi)+2*sum(log(diag(U)));   % normalization constant
118 y = -(c+q)/2;
119
120 function s = logsumexp(x, dim)
121 % Compute log(sum(exp(x),dim)) while avoiding numerical underflow.
122 %   By default dim = 1 (columns).
123 % Written by Michael Chen (sth4nth@gmail.com).
124 if nargin == 1,
125     % Determine which dimension sum will use
126     dim = find(size(x)≠1,1);
127     if isempty(dim), dim = 1; end
128 end
129
130 % subtract the largest in each column
131 y = max(x,[],dim);
132 x = bsxfun(@minus,x,y);
133 s = y + log(sum(exp(x),dim));
134 i = find(¬isfinite(y));
135 if ¬isempty(i)
136     s(i) = y(i);
137 end
```

References

[1] G. T. Carter, "Rehabilitation management in neuromuscular disease," *Journal of Neurologic Rehabilitation*, vol. 11, no. 2, pp. 69–80, 1997.

[2] N. Birbaumer, "Breaking the silence: Brain-computer interfaces (BCI) for communication and motor control," *Psychophysiology*, vol. 43, no. 6, pp. 517–532, 2006.

[3] G. Bauer, F. Gerstenbrand, and E. Rumpl, "VARIETIES OF THE LOCKED-IN SYNDROME," *Journal of Neurology*, vol. 221, no. 2, pp. 77–91, 1979.

[4] J. R. Wolpaw, N. Birbaumer, D. J. McFarland, G. Pfurtscheller, and T. M. Vaughan, "Brain-computer interfaces for communication and control," *Clinical Neurophysiology*, vol. 113, no. 6, pp. 767–791, 2002.

[5] F. Galan, M. Nuttin, E. Lew, P. W. Ferrez, G. Vanacker, J. Philips, and J. d. R. Millan, "A brain-actuated wheelchair: Asynchronous and non-invasive Brain-computer interfaces for continuous control of robots," *Clinical Neurophysiology*, vol. 119, no. 9, pp. 2159–2169, 2008.

[6] M. Velliste, S. Perel, M. C. Spalding, A. S. Whitford, and A. B. Schwartz, "Cortical control of a prosthetic arm for self-feeding," *Nature*, vol. 453, pp. 1098–1101, June 2008.

[7] N. Birbaumer, N. Ghanayim, T. Hinterberger, I. Iversen, B. Kotchoubey, A. Kubler, J. Perelmouter, E. Taub, and H. Flor, "A spelling device for the paralysed," *Nature*, vol. 398, no. 6725, pp. 297–298, 1999.

[8] J. Wolpaw, N. Birbaumer, W. Heetderks, D. McFarland, P. Peckham, G. Schalk, E. Donchin, L. Quatrano, C. Robinson, and T. Vaughan, "Brain-computer interface technology: a review of the first international meeting," *Rehabilitation Engineering, IEEE Transactions on*, vol. 8, no. 2, pp. 164–173, 2000.

[9] G. Pfurtscheller and C. Neuper, "Motor imagery activates primary sensorimotor area in humans," *Neuroscience Letters*, vol. 239, no. 2-3, pp. 65–68, 1997.

[10] D. J. McFarland, L. A. Miner, T. M. Vaughan, and J. R. Wolpaw, "Mu and beta rhythm topographies during motor imagery and actual movements," *Brain Topography*, vol. 12, no. 3, pp. 177–186, 2000.

[11] L. Farwell and E. Donchin, "Talking off the top of your head: toward a mental prosthesis utilizing event-related brain potentials," *Electroencephalography and Clinical Neurophysiology*, vol. 70, no. 6, pp. 510 – 523, 1988.

[12] S. P. Levine, J. E. Huggins, S. L. BeMent, R. K. Kushwaha, L. A. Schuh, E. A. Passaro, M. M. Rohde, and D. A. Ross, "Identification of electrocorticogram patterns as the basis for a direct brain interface," *Journal of Clinical Neurophysiology*, vol. 16, no. 5, pp. 439–447, 1999.

[13] L. F. Nicolas-Alonso and J. Gomez-Gil, "Brain Computer Interfaces, a Review," *Sensors*, vol. 12, pp. 1211–1279, Feb. 2012.

[14] H. H. Jasper, "The ten-twenty electrode system of the International Federation," *Electroencephalography and Clinical Neurophysiology*, no. 10, pp. 371–375, 1958.

[15] J. Dien, "Issues in the application of the average reference: Review, critiques, and recommendations," *Behavior Research Methods*, vol. 30, pp. 34–43, 1998. 10.3758/BF03209414.

[16] J. Yin, D. Jiang, and J. Hu, "Design and application of brain-computer interface web browser based on VEP," in *BioMedical Information Engineering, 2009. FBIE 2009. International Conference on Future*, pp. 77–80, 2009.

[17] X. Gao, D. Xu, M. Cheng, and S. Gao, "A BCI-based environmental controller for the motion-disabled," *Neural Systems and Rehabilitation Engineering, IEEE Transactions on*, vol. 11, no. 2, pp. 137–140, 2003.

[18] J. V. Odom, M. Bach, C. Barber, M. Brigell, M. F. Marmor, A. P. Tormene, G. E. Holder, and Vaegan, "Visual evoked potentials standard (2004)," *Documenta Ophthalmologica*, vol. 108, pp. 115–123, 2004. 10.1023/B:DOOP.0000036790.67234.22.

[19] Y. Wang, R. Wang, X. Gao, B. Hong, and S. Gao, "A practical VEP-based brain-computer interface," *Neural Systems and Rehabilitation Engineering, IEEE Transactions on*, vol. 14, no. 2, pp. 234–240, 2006.

[20] N. Birbaumer, "Slow cortical potentials: their origin, meaning, and clinical use," *Brain and Behavior Past, Present, and Future*, pp. 25–39, 1997.

[21] N. Birbaumer, "Slow cortical potentials: Plasticity, operant control, and behavioral effects," *The Neuroscientist*, vol. 5, no. 2, pp. 74–78, 1999.

[22] T. Hinterberger, S. Schmidt, N. Neumann, J. Mellinger, B. Blankertz, G. Curio, and N. Birbaumer, "Brain-computer communication and slow cortical potentials," *Biomedical Engineering, IEEE Transactions on*, vol. 51, no. 6, pp. 1011–1018, 2004.

[23] A. Kubler, F. Nijboer, J. Mellinger, T. M. Vaughan, H. Pawelzik, G. Schalk, D. J. McFarland, N. Birbaumer, and J. R. Wolpaw, "Patients with ALS can use sensorimotor rhythms to operate a brain-computer interface," *Neurology*, vol. 64, no. 10, pp. 1775–1777, 2005.

[24] G. Pfurtscheller, C. Neuper, H. Ramoser, and J. Muller-Gerking, "Visually guided motor imagery activates sensorimotor areas in humans," *Neuroscience Letters*, vol. 269, no. 3, pp. 153–156, 1999.

[25] C. Guger, S. Daban, E. Sellers, C. Holzner, G. Krausz, R. Carabalona, F. Gramatica, and G. Edlinger, "How many people are able to control a P300-based braincomputer interface (BCI)?," *Neuroscience Letters*, vol. 462, pp. 94–98, Sept. 2009.

[26] M. Thulasidas, C. Guan, and J. Wu, "Robust classification of EEG signal for brain-computer interface," *Neural Systems and Rehabilitation Engineering, IEEE Transactions on*, vol. 14, no. 1, pp. 24–29, 2006.

[27] F. Piccione, F. Giorgi, P. Tonin, K. Priftis, S. Giove, S. Silvoni, G. Palmas, and F. Beverina, "P300-based brain computer interface: Reliability and performance in healthy and paralysed participants," *Clinical Neurophysiology*, vol. 117, pp. 531–537, Mar. 2006.

[28] G. R. Muller-Putz, R. Scherer, C. Brauneis, and G. Pfurtscheller, "Steady-state visual evoked potential (SSVEP)-based communication: impact of harmonic frequency components.," *Journal of neural engineering*, vol. 2, pp. 123–30, Dec. 2005.

[29] M. Cheng, X. Gao, S. Gao, and D. Xu, "Design and implementation of a brain-computer interface with high transfer rates," *Biomedical Engineering, IEEE Transactions on*, vol. 49, no. 10, pp. 1181–1186, 2002.

[30] I. Volosyak, "SSVEP-based Bremen-BCI interface-boosting information transfer rates," *Journal of Neural Engineering*, vol. 8, p. 036020, June 2011.

[31] S. Kelly, E. Lalor, R. Reilly, and J. Foxe, "Visual spatial attention tracking using high-density SSVEP data for independent brain-computer communication," *Neural Systems and Rehabilitation Engineering, IEEE Transactions on*, vol. 13, no. 2, pp. 172–178, 2005.

[32] J. Wolpaw, D. McFarland, G. Neat, and C. Forneris, "An EEG-based brain-computer interface for cursor control," *Electroencephalography and clinical neurophysiology*, vol. 78, no. 3, pp. 252–259, 1991.

[33] D. McFarland, A. Lefkowicz, and J. Wolpaw, "Design and operation of an EEG-based brain-computer interface with digital signal processing technology," *Behavior research methods*, vol. 29, no. 3, pp. 337–345, 1997.

[34] C. Neuper, G. Muller, K. R.ller-Putz, R. Scherer, and G. Pfurtscheller, "Motor imagery and EEG-based control of spelling devices and neuroprostheses.," *Progress in brain research*, vol. 159, p. 393, 2006.

[35] G. Schalk, E. C. Leuthardt, P. Brunner, J. G. Ojemann, L. A. Gerhardt, and J. R. Wolpaw, "Real-time detection of event-related brain activity," *Neuroimage*, vol. 43, no. 2, pp. 245–249, 2008.

[36] A. Dempster, N. Laird, and D. Rdin, "Maximum Likelihood from Incomplete Data via the EM Algorithm," in *JOURNAL OF THE ROYAL STATISTICAL SOCIETY, SERIES B*, vol. 39, pp. 1–38, 1977.

[37] T. K. Moon, "The expectation-maximization algorithm," *Ieee Signal Processing Magazine*, vol. 13, no. 6, pp. 47–60, 1996.

[38] Y. Chen and M. Gupta, "Em demystified: An expectation-maximization tutorial," *Electrical Engineering*, vol. 206, 2010.

[39] R. Kalman, "A new approach to linear filtering and prediction problems," *Journal of basic Engineering*, vol. 82, no. 1, pp. 35–45, 1960.

[40] M. Khan and D. Dutt, "An expectation-maximization algorithm based Kalman smoother approach for event-related desynchronization (ERD) estimation from EEG," *Biomedical Engineering, IEEE Transactions on*, vol. 54, no. 7, pp. 1191–1198, 2007.

[41] A. Tzovara, M. M. Murray, G. Plomp, M. H. Herzog, C. M. Michel, and M. De Lucia, "Decoding stimulus-related information from single-trial EEG responses based on voltage topographies," *Pattern Recognition*, vol. 45, pp. 2109–2122, June 2012.

[42] L. Meng, M. G. Frei, I. Osorio, G. Strang, and T. Q. Nguyen, "Gaussian mixture models of ECoG signal features for improved detection of epileptic seizures," *Medical Engineering & Physics*, vol. 26, pp. 379–393, June 2004.

[43] S. Makeig, S. Debener, J. Onton, and A. Delorme, "Mining event-related brain dynamics," *Trends in Cognitive Sciences*, vol. 8, no. 5, pp. 204–210, 2004.

[44] A. Delorme and S. Makeig, "EEGLAB: an open source toolbox for analysis of single-trial EEG dynamics including independent component analysis," *Journal of Neuroscience Methods*, vol. 134, pp. 9–21, Mar. 2004.

[45] C. Tallon-Baudry, O. Bertrand, C. Delpuech, and J. Pernier, "Stimulus specificity of phase-locked and non-phase-locked 40 Hz visual responses in human," *The Journal of Neuroscience*, vol. 16, no. 13, pp. 4240–4249, 1996.

[46] V. J. Samar, A. Bopardikar, R. Rao, and K. Swartz, "Wavelet analysis of neuroelectric waveforms: A conceptual tutorial," *Brain and Language*, vol. 66, no. 1, pp. 7–60, 1999.

[47] G. Strang, "WAVELET TRANSFORMS VERSUS FOURIER-TRANSFORMS," *Bulletin of the American Mathematical Society*, vol. 28, no. 2, pp. 288–305, 1993.

[48] S. J. Schiff, A. Aldroubi, M. Unser, and S. Sato, "FAST WAVELET TRANSFORMATION OF EEG," *Electroencephalography and Clinical Neurophysiology*, vol. 91, no. 6, pp. 442–455, 1994.

[49] J. Raz, L. Dickerson, and B. Turetsky, "A wavelet packet model of evoked potentials," *Brain and Language*, vol. 66, no. 1, pp. 61–88, 1999.

[50] W.-Y. Hsu and Y.-N. Sun, "EEG-based motor imagery analysis using weighted wavelet transform features," *Journal of Neuroscience Methods*, vol. 176, pp. 310–318, Jan. 2009.

[51] T. Demiralp, A. Ademoglu, M. Schrmann, C. Basar-Eroglu, and E. Basar, "Detection of P300 Waves in Single Trials by the Wavelet Transform (WT)," *Brain and Language*, vol. 66, pp. 108–128, Jan. 1999.

[52] G. Valsan, *Brain Computer Interface Using Detection of Movement Intention.* PhD thesis, Bioengineering Department, University of Strathclyde, 2007.

[53] C. M. Bishop, *Pattern Recognition and Machine Learning (Information Science and Statistics).* Springer-Verlag New York, Inc., 2006.

[54] M. Chen, "EM algorithm for Gaussian mixture model (Matlab Code)," 2009. This is an electronic document. Date of publication: December 23, 2009. Date retrieved: October 21, 2012. Date last modified: February 29, 2012.

[55] S. L. Morgan, "Guide to Microsoft Excel for calculations, statistics, and plotting data," 2006. This is an electronic document. Date of publication: [Date unavailable]. Date retrieved: October 10, 2012. Date last modified: June 7, 2006.

[56] G. Schalk, P. Brunner, L. Gerhardt, H. Bischof, and J. Wolpaw, "Brain Computer Interfaces (BCIs): Detection instead of classification," *Journal of Neuroscience Methods*, vol. 167, pp. 51–62, Jan. 2008.

[57] G. Pfurtscheller and C. Neuper, "Future prospects of ERD/ERS in the context of brain computer interface (BCI) developments," *Progress in brain research*, vol. 159, pp. 433–437, 2006.

[58] C. Neuper, R. Scherer, S. Wriessnegger, and G. Pfurtscheller, "Motor imagery and action observation: modulation of sensorimotor brain rhythms during mental control of a braincomputer interface," *Clinical neurophysiology*, vol. 120, no. 2, p. 239, 2009.

[59] H. Lakany and B. Conway, "Understanding intention of movement from electroencephalograms," *Expert Systems*, vol. 24, no. 5, pp. 295–304, 2007.

[60] L. Deecke, P. Scheid, and H. Kornhuber, "Distribution of readiness potential, pre-motion positivity, and motor potential of the human cerebral cortex preceding voluntary finger movements," 1969-01-17.

[61] G. Pfurtscheller and C. Neuper, "Future prospects of ERD/ERS in the context of braincomputer interface (BCI) developments," in *Event-Related Dynamics of Brain Oscillations* (C. Neuper and W. Klimesch, eds.), vol. Volume 159, pp. 433–437, Elsevier, 2006.

[62] G. Pfurtscheller, M. Pregenzer, and C. Neuper, "Visualization of sensorimotor areas involved in preparation for hand movement based on classification of and central rhythms in single EEG trials in man," *Neuroscience Letters*, vol. 181, pp. 43–46, Nov. 1994.

[63] J. ygierewicz, P. Durka, H. Klekowicz, P. Franaszczuk, and N. Crone, "Computationally efficient approaches to calculating significant ERD/ERS changes in the timefrequency plane," *Journal of Neuroscience Methods*, vol. 145, pp. 267–276, June 2005.

[64] . Ar, S. Aksoy, and O. Arkan, "Maximum likelihood estimation of Gaussian mixture models using stochastic search," *Pattern Recognition*, 2012.

[65] C. Tallon-Baudry and O. Bertrand, "Oscillatory gamma activity in humans and its role in object representation," *Trends in cognitive sciences*, vol. 3, no. 4, pp. 151–162, 1999.